tamarins followed by recovery to the initial levels at around 2 weeks after administration, while the cells were maintained at the initial levels in the monkeys with MOPC-21 (Fig. 2a). In addition, it is noteworthy that the ratios of CD4$^+$ and CD8$^+$ T cells and CD20$^+$ B cells were not affected by the administration of the 3G8 mAb (Supplementary Figure 1). In the case of administration of mAb MOPC-21, we confirmed no significant effect on CD16$^+$ cells (Supplementary Figure 2). The killing activities of the peripheral blood mononuclear cells (PBMCs) taken from the 3G8-treated monkeys were reduced at day 1 post-antibody-treatment, followed by an increase irrespective of depletion of CD16$^+$ NK cells at day 2 post-antibody-treatment (1 day after DENV inoculation), suggesting that the CD16$^-$ NK population may be activated by DENV infection (Fig. 2b). Plasma viral loads in both mAb-treated monkeys rose to 10^5 copies/ml by day 1 after infection and then reached a peak at 10^6 copies/ml on day 3 or day 7, followed by a rapid decline, with values dipping below the detectable level by day 14 after infection (Fig. 2c). These results suggested that CD16$^+$ NK cells apparently did not contribute to DENV replication in the acute phase in our tamarin model.

It was reported previously that non-structural glycoprotein NS1 is essential for flavivirus viability and that the NS1 protein circulates during the acute phase of disease in the plasma of patients infected with DENV [1]. Epidemiological studies have demonstrated that secreted NS1 levels are correlated with viremia levels and are higher in cases of DHF than in dengue fever (DF) early in illness [16]. Thus, it has been suggested that NS1 might be a useful marker as an indicator of the severity of dengue disease. We have used the level of the NS1 antigen as an alternative diagnostic marker to examine the effects of CD16 antibody treatment on DENV replication. The NS1 was measured by Platelia Dengue NS1 Ag assay (BioRad). Antigenemia was observed in these infected monkeys between 3-14 days post-infection. Serum IgM and IgG specific for DENV antigens were measured by ELISA. DENV-specific IgM or IgG antibody was equally detected in both mAb-treated monkeys (Fig. 3).

We recently demonstrated that marmosets are permissive to DENV infection [22]. In this study, we found that tamarins are also permissive to DENV infection (Fig. 1). Moreover, we also investigated the role of NK cells against early DENV infection using *in vivo* depletion of CD16$^+$

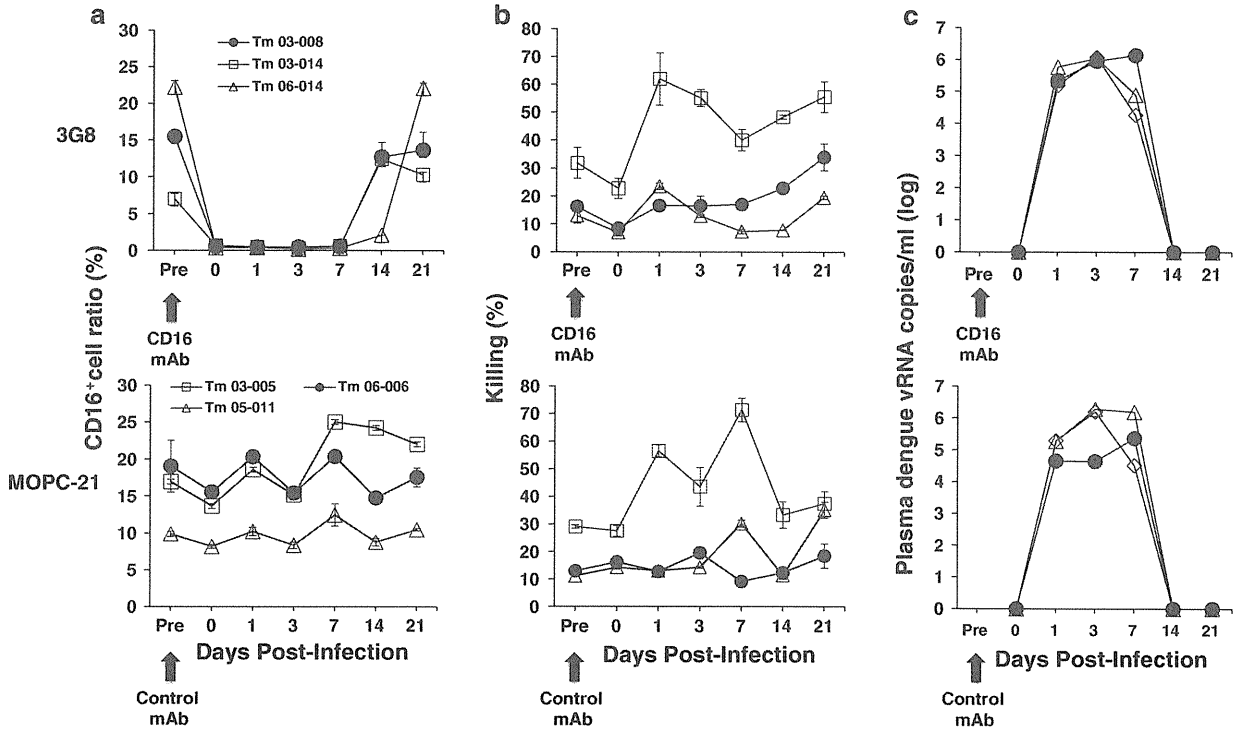

Fig. 2 Ratios of CD16$^+$ NK cells, killing activity of PBMCs, and vRNA in DENV-infected tamarins after treatment with 3G8 or MOPC-21 mAb. Tamarins were infected subcutaneously with DENV at a dose $3x10^5$ PFU/ml after treatment with 50 mg/kg of 3G8 or MOPC-21 mAb. **a** Ratios of CD16$^+$ NK cells were determined in whole-blood specimens. **b** The activities of NK cells were determined in PBMCs of tamarins by NK cytotoxic assay. **c** The vRNAs were detected in plasma by real-time PCR

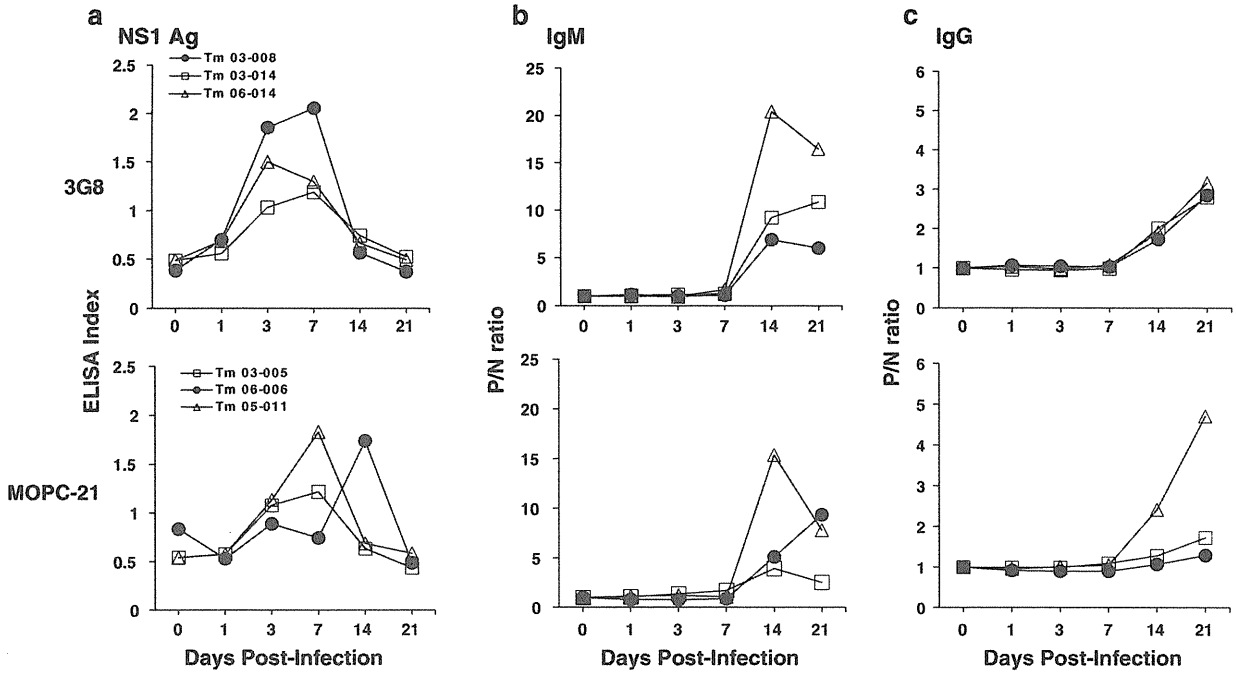

Fig. 3 Levels of NS1 antigen and DENV-specific IgM and IgG in plasma samples from DENV-infected tamarins after treatment with 3G8 or MOPC-21 mAb. The levels of NS1 antigen and DENV-specific IgM and IgG in plasma were measured by ELISA. **a** ELISA index of NS1 antigen, **b** positive/negative (P/N) ratio of DENV-specific IgM, **c** P/N ratio of DENV-specific IgG in plasma samples from DENV-infected tamarins after administration of the 3G8 or MOPC-21 mAb. The P/N ratio was calculated as the optical density of the test sample divided by that of a negative sample. P/N ratios <2 and ≥ 2 were considered to be negative and positive, respectively. Top, 3G8; bottom, MOPC-21 mAb

NK cells in tamarins and found that the depletion of $CD16^+$ NK cells had almost no effect on DENV replication (Fig. 2), indicating that this NK subpopulation is unlikely to contribute to controlling DENV replication. Interestingly, these results imply that the $CD16^-$ NK subpopulation may have a critical role of controlling DENV infection *in vivo*.

Using our model, we investigated the role of NK cells *in vivo* against DENV infection, which remains to be elucidated in several aspects. We previously reported that almost complete *in vivo* depletion of the $CD16^+$ NK subpopulation was not able to completely remove the NK-mediated cytotoxic activity in tamarins [29]. In this study, despite a transient but substantial reduction in the $CD16^+$ NK cell number following 3G8 treatment in tamarins, DENV replication was comparable to that in monkeys that received the control mAb. The NK-mediated cytotoxic activity was augmented in both study groups, indicating that $CD16^-$ NK cells were responsible for the cytotoxic activity and suggesting that they might play a role in controlling DENV replication.

The next question is how $CD16^-$ NK cells may regulate DENV infection. One possibility regarding $CD16^-$ NK cells is that $CD56^+$ or $CD57^+$ NK cells are involved in controlling DENV infection. Human NK cells are classically divided into two functional subsets based on their cell-surface density of CD56 and CD16, i.e., $CD56^{bright}CD16^-$ immunoregulatory cells and $CD56^{dim}CD16^+$ cytotoxic cells. Both subsets have been characterized extensively regarding their different functions, phenotypes, and tissue localization [8]. The NK cell number is maintained by a continuous differentiation process associated with the expression of CD57 that results in NK cells with poor responsiveness to cytokine stimulation but high cytolytic capacity [3, 18]. The second possibility is that $CD16^-$ NK cells have a non-cytolytic helper function. Generally, it is well known that NK cells possess both a cytolytic and a non-cytolytic helper function. It has been suggested that cytokine production is carried out by $CD56^{bright}CD16^-$ NK cells [4–6]. Interferon (IFN)-γ secreted by NK cells has shown potent antiviral effects against DENV infection in early phases [25]. One aspect of the NK helper function arises from recent evidence indicating that NK cells can be induced to function as non-cytotoxic helper cells following stimulation with interleukin-18 [19]. This cytokine induces IFN-γ secretion from NK cells and thus enables dendritic cells (DCs) to secrete IL-12, leading to Th1 polarization [19]. It is possible that $CD16^-$ NK cells, which have poor

cytotoxic activity but an enhanced ability to secrete cytokines and then lead to a Th1 response, are preserved during 3G8 administration. The persistence of this minor CD16$^-$ NK cell subpopulation could exert an antiviral effect through INF-γ-mediated pathways despite the depletion of CD16$^+$ NK cells. The third possibility is that CD16$^+$ NK cells of tamarins play pivotal roles against bacterial infections and cancer progression but not DENV-infected cells. We will address these possibilities for the roles of the NK subpopulation in the future studies.

In conclusion, this study provides a DENV *in vivo* replication model in tamarins and new information on the possible role of CD16$^+$ NK cells in DENV replication *in vivo*. It remains elusive whether the CD16$^+$ and CD16$^-$ NK subpopulations could play an important role in the control of primary DENV infection.

Acknowledgments We would like to give special thanks to members of the Corporation for Production and Research of Laboratory Primates for technical assistance. We also would like to give special thanks to Ms. Tomoko Ikoma and Ms. Mizuho Fujita for technical assistance. Moreover, we appreciate Dr. Keith A. Reimann (the NIH Nonhuman Primate Reagent Resource R24 RR016001, NIAID contact HHSN272200900037C) for providing CD16 antibody. This work was supported by grants from the Ministry of Health, Labor and Welfare of Japan (to Hirofumi Akari and Ichiro Kurane). This research was also supported by the Environment Research and Technology Development Fund (D-1007) from the Ministry of the Environment of Japan (to Tomoyuki Yoshida and Hirofumi Akari).

Conflict of interest The authors declare that the research was conducted in the absence of any commercial or financial relationships that could be construed as a potential conflict of interest.

References

1. Alcon-LePoder S, Sivard P, Drouet MT, Talarmin A, Rice C, Flamand M (2006) Secretion of flaviviral non-structural protein NS1: from diagnosis to pathogenesis. Novartis Found Symp 277:233–247 (discussion 247–253)
2. Azeredo EL, De Oliveira-Pinto LM, Zagne SM, Cerqueira DI, Nogueira RM, Kubelka CF (2006) NK cells, displaying early activation, cytotoxicity and adhesion molecules, are associated with mild dengue disease. Clin Exp Immunol 143:345–356
3. Bjorkstrom NK, Riese P, Heuts F, Andersson S, Fauriat C, Ivarsson MA, Bjorklund AT, Flodstrom-Tullberg M, Michaelsson J, Rottenberg ME, Guzman CA, Ljunggren HG, Malmberg KJ (2010) Expression patterns of NKG2A, KIR, and CD57 define a process of CD56dim NK-cell differentiation uncoupled from NK-cell education. Blood 116:3853–3864
4. Caligiuri MA (2008) Human natural killer cells. Blood 112: 461–469
5. Cooper MA, Fehniger TA, Turner SC, Chen KS, Ghaheri BA, Ghayur T, Carson WE, Caligiuri MA (2001) Human natural killer cells: a unique innate immunoregulatory role for the CD56(bright) subset. Blood 97:3146–3151
6. Farag SS, Caligiuri MA (2006) Human natural killer cell development and biology. Blood Rev 20:123–137
7. Fleit HB, Wright SD, Unkeless JC (1982) Human neutrophil Fc gamma receptor distribution and structure. Proc Natl Acad Sci USA 79:3275–3279
8. Gayoso I, Sanchez-Correa B, Campos C, Alonso C, Pera A, Casado JG, Morgado S, Tarazona R, Solana R (2011) Immunosenescence of human natural killer cells. J Innate Immun 3:337–343
9. Green S, Pichyangkul S, Vaughn DW, Kalayanarooj S, Nimmannitya S, Nisalak A, Kurane I, Rothman AL, Ennis FA (1999) Early CD69 expression on peripheral blood lymphocytes from children with dengue hemorrhagic fever. J Infect Dis 180:1429–1435
10. Guzman MG, Kouri G, Valdes L, Bravo J, Alvarez M, Vazques S, Delgado I, Halstead SB (2000) Epidemiologic studies on Dengue in Santiago de Cuba, 1997. Am J Epidemiol 152: 793–799 (discussion 804)
11. Halstead SB, Lan NT, Myint TT, Shwe TN, Nisalak A, Kalyanarooj S, Nimmannitya S, Soegijanto S, Vaughn DW, Endy TP (2002) Dengue hemorrhagic fever in infants: research opportunities ignored. Emerg Infect Dis 8:1474–1479
12. Halstead SB (2007) Dengue. Lancet 370:1644–1652
13. Hershkovitz O, Rosental B, Rosenberg LA, Navarro-Sanchez ME, Jivov S, Zilka A, Gershoni-Yahalom O, Brient-Litzler E, Bedouelle H, Ho JW, Campbell KS, Rager-Zisman B, Despres P, Porgador A (2009) NKp44 receptor mediates interaction of the envelope glycoproteins from the West Nile and dengue viruses with NK cells. J Immunol 183:2610–2621
14. Kurane I, Hebblewaite D, Ennis FA (1986) Characterization with monoclonal antibodies of human lymphocytes active in natural killing and antibody-dependent cell-mediated cytotoxicity of dengue virus-infected cells. Immunology 58:429–436
15. Lee SH, Miyagi T, Biron CA (2007) Keeping NK cells in highly regulated antiviral warfare. Trends Immunol 28:252–259
16. Libraty DH, Young PR, Pickering D, Endy TP, Kalayanarooj S, Green S, Vaughn DW, Nisalak A, Ennis FA, Rothman AL (2002) High circulating levels of the dengue virus nonstructural protein NS1 early in dengue illness correlate with the development of dengue hemorrhagic fever. J Infect Dis 186:1165–1168
17. Libraty DH, Acosta LP, Tallo V, Segubre-Mercado E, Bautista A, Potts JA, Jarman RG, Yoon IK, Gibbons RV, Brion JD, Capeding RZ (2009) A prospective nested case-control study of Dengue in infants: rethinking and refining the antibody-dependent enhancement dengue hemorrhagic fever model. PLoS Med 6:e1000171
18. Lopez-Verges S, Milush JM, Pandey S, York VA, Arakawa-Hoyt J, Pircher H, Norris PJ, Nixon DF, Lanier LL (2010) CD57 defines a functionally distinct population of mature NK cells in the human CD56dimCD16+ NK-cell subset. Blood 116:3865–3874
19. Mailliard RB, Alber SM, Shen H, Watkins SC, Kirkwood JM, Herberman RB, Kalinski P (2005) IL-18-induced CD83+CCR7+ NK helper cells. J Exp Med 202:941–953
20. Mathew A, Rothman AL (2008) Understanding the contribution of cellular immunity to dengue disease pathogenesis. Immunol Rev 225:300–313
21. Navarro-Sanchez E, Despres P, Cedillo-Barron L (2005) Innate immune responses to dengue virus. Arch Med Res 36:425–435
22. Omatsu T, Moi ML, Hirayama T, Takasaki T, Nakamura S, Tajima S, Ito M, Yoshida T, Saito A, Katakai Y, Akari H, Kurane I (2011) Common marmoset (Callithrix jacchus) as a primate model of dengue virus infection: development of high levels of viremia and demonstration of protective immunity. J Gen Virol 92:2271–2280. doi:10.1099/vir.0.031229-0
23. Scalzo AA, Corbett AJ, Rawlinson WD, Scott GM, Degli-Esposti MA (2007) The interplay between host and viral factors in shaping the outcome of cytomegalovirus infection. Immunol Cell Biol 85:46–54
24. Shresta S, Kyle JL, Robert Beatty P, Harris E (2004) Early activation of natural killer and B cells in response to primary dengue virus infection in A/J mice. Virology 319:262–273

25. Suwannasaen D, Romphruk A, Leelayuwat C, Lertmemongkolchai G (2010) Bystander T cells in human immune responses to dengue antigens. BMC Immunol 11:47
26. Vaughn DW, Green S, Kalayanarooj S, Innis BL, Nimmannitya S, Suntayakorn S, Endy TP, Raengsakulrach B, Rothman AL, Ennis FA, Nisalak A (2000) Dengue viremia titer, antibody response pattern, and virus serotype correlate with disease severity. J Infect Dis 181:2–9
27. Wahid SF, Sanusi S, Zawawi MM, Ali RA (2000) A comparison of the pattern of liver involvement in dengue hemorrhagic fever with classic dengue fever. Southeast Asian J Trop Med Public Health 31:259–263
28. Woollard DJ, Haqshenas G, Dong X, Pratt BF, Kent SJ, Gowans EJ (2008) Virus-specific T-cell immunity correlates with control of GB virus B infection in marmosets. J Virol 82:3054–3060
29. Yoshida T, Saito A, Iwasaki Y, Iijima S, Kurosawa T, Katakai Y, Yasutomi Y, Reimann KA, Hayakawa T, Akari H (2010) Characterization of natural Killer cells in tamarins: a technical basis for studies of innate immunity. Front Microbiol 1:128. doi: 10.3389/fmicb.2010.00128

frontiers in
MICROBIOLOGY

ORIGINAL RESEARCH ARTICLE
published: 07 December 2011
doi: 10.3389/fmicb.2011.00240

Long-term persistent GBV-B infection and development of a chronic and progressive hepatitis C-like disease in marmosets

Yuki Iwasaki[1,2†], Ken-ichi Mori[3†], Koji Ishii[4], Noboru Maki[3], Sayuki Iijima[1], Tomoyuki Yoshida[5], Sachi Okabayashi[6], Yuko Katakai[6], Young-Jung Lee[1], Akatsuki Saito[5], Hiromi Fukai[3], Nobuyuki Kimura[1], Naohide Ageyama[1], Sayaka Yoshizaki[4], Tetsuro Suzuki[4], Yasuhiro Yasutomi[1], Tatsuo Miyamura[4], Mari Kannagi[2] and Hirofumi Akari[1,5]*

[1] Tsukuba Primate Research Center, National Institute of Biomedical Innovation, Tsukuba, Japan
[2] Department of Immunotherapeutics, Graduate School of Medicine and Dentistry, Tokyo Medical and Dental University, Tokyo, Japan
[3] Advanced Life Science Institute, Wako, Japan
[4] Department of Virology II, National Institute of Infectious Diseases, Tokyo, Japan
[5] Primate Research Institute, Kyoto University, Inuyama, Japan
[6] Corporation for Production and Research of Laboratory Primates, Tsukuba, Japan

Edited by:
Yasuko Yokota, National Institute of Infectious Diseases, Japan

Reviewed by:
Ikuo Shoji, Kobe University Graduate School of Medicine, Japan
Soon B. Hwang, Hallym University, South Korea

***Correspondence:**
Hirofumi Akari, Primate Research Institute, Kyoto University, Inuyama 484-8506, Japan.
e-mail: akari@pri.kyoto-u.ac.jp

†Yuki Iwasaki and Ken-ichi Mori have contributed equally to this work.

It has been shown that infection of GB virus B (GBV-B), which is closely related to hepatitis C virus, develops acute self-resolving hepatitis in tamarins. In this study we sought to examine longitudinally the dynamics of viral and immunological status following GBV-B infection of marmosets and tamarins. Surprisingly, two of four marmosets but not tamarins experimentally challenged with GBV-B developed long-term chronic infection with fluctuated viremia, recurrent increase of alanine aminotransferase and plateaued titers of the antiviral antibodies, which was comparable to chronic hepatitis C in humans. Moreover, one of the chronically infected marmosets developed an acute exacerbation of chronic hepatitis as revealed by biochemical, histological, and immunopathological analyses. Of note, periodical analyses of the viral genomes in these marmosets indicated frequent and selective non-synonymous mutations, suggesting efficient evasion of the virus from antiviral immune pressure. These results demonstrated for the first time that GBV-B could induce chronic hepatitis C-like disease in marmosets and that the outcome of the viral infection and disease progression may depend on the differences between species and individuals.

Keywords: GBV-B, HCV, marmoset, tamarin, hepatitis C

INTRODUCTION

Among the known viruses, GB virus B (GBV-B) is closely related to hepatitis C virus (HCV), with 25–30% homology at the amino acid level, and is tentatively classified in *Hepacivirus* genus of *Flavivirus* family (Muerhoff et al., 1995; Simons et al., 1995; Ohba et al., 1996). Due to limited epidemiological analyses, the natural host(s) and prevalence of GBV-B have remained to be determined.

Hepatitis C virus is a major causative agent for non-A, non-B hepatitis. HCV is globally disseminated and estimated to be carried by more than 170 million people (Chisari, 2005; Lavanchy, 2009). Most HCV-infected individuals develop chronic liver diseases such as liver cirrhosis and hepatocellular carcinoma (Hoofnagle, 1997; Seeff and Hoofnagle, 2002; Rehermann and Nascimbeni, 2005). Since standard therapy with PEGylated interferon and ribavirin is effective for only about 50% of patients, it is crucial to develop more effective therapeutics (Feld and Hoofnagle, 2005; Melnikova, 2008). The only validated animal model for HCV infection is the chimpanzees. This model has been valuable for determining important aspects of this disease, including the relationship between the virus and the antiviral immune responses of the host and the process of viral pathogenesis (Bukh, 2004; Akari et al., 2009; Boonstra et al., 2009). However, chimpanzees are endangered and present ethical complications and the availability of these experimental animals is severely restricted.

When tamarins (members of the New World monkeys) are infected with GBV-B, they generally develop acute viremia and self-resolving hepatitis as indicated by increases in the levels of serum enzymes such as alanine aminotransferase (ALT) (Bukh et al., 1999; Beames et al., 2000; Beames et al., 2001; Sbardellati et al., 2001; Lanford et al., 2003; Martin et al., 2003; Bright et al., 2004; Jacob et al., 2004; Nam et al., 2004; Kyuregyan et al., 2005; Ishii et al., 2007; Weatherford et al., 2009). Thus, the monkeys have been proposed as a surrogate model of HCV infection of chimpanzee and humans. However, a major hurdle for the development of a monkey-based surrogate model is the difficulties encountered in obtaining chronically infected monkeys that exhibit progression of chronic hepatitis C-like diseases (Martin et al., 2003; Nam et al., 2004; Takikawa et al., 2010).

Abbreviations: ALT, alanine aminotransferase; GBV-B, GB virus B; HCV, hepatitis C virus; HE, hematoxylin and eosin; p.i., post infection.

It has recently been shown that marmosets, another member of New World monkeys, are susceptible to GBV-B infection and develop relatively lower levels of acute viremia (10^5–10^8 copies/ml) as compared with that in tamarins (10^7–10^{10} copies/ml) (Lanford et al., 2003; Bright et al., 2004; Woollard et al., 2008; Weatherford et al., 2009), although it remains elusive whether the marmosets could permit persistent GBV-B infection. Considering that the viral loads in the acute phase of experimental HCV infection of chimpanzees that consequently develop persistent infection are generally 10^7 copies/ml or less (Fernandez et al., 2004; Bukh et al., 2008), it is possible that the lower viral loads in the acute phase is preferable for the establishment of viral persistency. We thus initiated studies of the dynamics of viral and immunological status following GBV-B infection of tamarins and marmosets in a longitudinal follow-up study. We show here for the first time that GBV-B infection produces a chronic and progressive hepatitis C-like disease in marmosets as demonstrated by fibrosis and a recurrent ALT increase and that one of the marmosets experienced acute exacerbation of chronic hepatitis as indicated by piecemeal necrosis and an ALT flare >4 years after infection.

MATERIALS AND METHODS

ANIMALS

Adult red-handed tamarins (*Saguinus midas*) and common marmosets (*Callithrix jacchus*) were housed in individual cages at the Tsukuba Primate Research Center. All animal studies were conducted in accordance with the protocols of experimental procedures that were approved by the Animal Welfare and Animal Care Committees of the National Institute of Biomedical Innovation and the National Institute of Infectious Diseases.

GBV-B INFECTION IN TAMARINS AND MARMOSETS

GBV-B infectious serum obtained from a tamarin (1.3×10^9 viral RNA copies per inoculum) was injected into each tamarin and marmoset intrahepatically as previously described (Ishii et al., 2007). We confirmed that the inoculum contained no mutations as compared with the original sequence. Of note, an anti-luciferase siRNA in a cationic liposome formulation was administered to one of the marmosets (Cj05-002) 2 days before the infection, which was performed as previously described (Yokota et al., 2007). Blood samples were periodically collected from the femoral vein of each animal under anesthesia and the plasma samples were evaluated for GBV-B genomic RNA, ALT, and antibodies against GBV-B core and NS3 proteins.

QUANTIFICATION OF GBV-B GENOMIC RNA

GBV-B RNA was isolated from the plasma samples by using a QIAamp MinElute Virus Spin kit (QIAGEN) and was quantified by real-time PCR using the 5′-exonuclease PCR (TaqMan) assay system (Ishii et al., 2007). The primers 558F [5′-AACGAGCAAAGCGCAAAGTC] and 626R [5′-CATCATGGATACCAGCAATTTTGT] and the probe 579P [5′-FAM-AGCGCGATGCTCGGCCTCGTA-TAMRA] (Beames et al., 2000) were obtained from Sigma-Aldrich. The cutoff value was 10^3 copies/ml. All the specimens were evaluated in duplicate and the average values were calculated.

DETECTION OF ANTIBODIES AGAINST GBV-B CORE AND NS3 PROTEINS BY ELISA

Tamarin and marmoset plasma samples were evaluated for anti-GBV-B core and NS3 antibodies by ELISA as described previously (Ishii et al., 2007).

HISTOPATHOLOGICAL AND IMMUNOHISTOCHEMICAL ANALYSES

Liver samples obtained by necropsy from the GBV-B-infected marmoset were examined histopathologically as previously described (Ishii et al., 2007). For standard histological examination, the sections were subjected to hematoxylin and eosin (HE) staining. Masson's trichrome staining was also performed to estimate the development of fibrosis according to a standard laboratory protocol. To detect the viral protein in tissues, we employed a mouse anti-core monoclonal antibody, 5A10, that we generated. In brief, Mice were immunized with the GBV-B core protein expressed in *E. coli* (Ishii et al., 2007). Hybridoma cells producing an anti-core mAb were screened by both the core-expressing 293T cells and the liver sections of an acutely GBV-B-infected tamarin. Liver samples were fixed in 10% neutral buffered formalin and embedded in paraffin wax. Sections were deparaffinized by pretreating with 0.5% periodic acid and then subjected to antigen retrieval with citric acid buffer and heating in an autoclave for 10 min at 121°C. The sections were then incubated free floating in primary antibody solution (5A10; 1:50 dilution) overnight at 4°C. Following brief washes with wash buffer, the sections were sequentially incubated with a biotinylated goat anti-mouse IgG (1:400 dilution), followed by addition of a streptavidin–biotin–horseradish peroxidase complex (sABC kit; DAKO, Denmark). Immunoreactive elements in the sections were visualized by treatment with 3,3′-diaminobenzidine tetroxide (Dojin Kagaku, Japan), together with counterstaining with hematoxylin.

DETERMINATION OF THE GBV-B SEQUENCE

Viral RNA was isolated from the plasma of GBV-B-infected marmosets as described above. GBV-B cDNA was synthesized using SuperScript reverse transcriptase III (Invitrogen) with random hexamer primers (Invitrogen). The resulting cDNAs were used to obtain PCR amplification products of lengths of 0.5–1.0 kb, using GBV-B-specific primers and LA-Taq DNA polymerase (TaKaRa). The PCR products were then purified from the gel using a QIA-quick gel extraction kit (QIAGEN), and the purified amplimers were sequenced directly using a CEQ-2000XL analysis system (Beckman) with a DTCS quick start kit and GBV-B-specific primers according to the manufacturer's instructions. Sequence data were analyzed using the Sequencher 4.8 (Gene Codes) and Mac Vector 10.6 (MacVector) software packages. The GenBank accession numbers of the viral genome sequences in each time point are as follows: AB630358, AB630359, and AB630360 for 45, 104, and 135 weeks after infection in Cj05-002; AB630361, AB630362, AB630363, and AB630364 for 33, 88, 141, and 229 weeks after infection in Cj05-004, respectively. Throughout this article, the amino acids are numbered according to the full-length genome sequence of isolate pGBB (GenBank accession number AF179612).

RESULTS

GBV-B INFECTION IN TAMARINS AND MARMOSETS

Four tamarins and four marmosets were intrahepatically inoculated with GBV-B and the growth kinetics and pathogenesis of the virus were compared. In tamarins, the peak viral loads in plasma reached 10^9–10^{10} copies/ml in the acute phase and the viremia was maintained for an average of 3 months in parallel with increases in plasma ALT levels (**Figure 1A**). Antibodies reactive with the viral core and NS3 proteins were developed in all of the tamarins as the plasma viral loads were reduced and the antibody titers reached maximum levels concurrently with the complete loss of detectable viral RNA (**Figure 1A**). In contrast, two of four marmosets infected with GBV-B developed chronic infection while the others exhibited a phenotype similar to that of the tamarins (i.e., subacute clearance of the viremia followed by antibody responses). One exception is that lower plasma viral loads (10^7–10^8 copies/ml) were observed in the marmosets relative to those of the tamarins (**Figure 1B**). The details of the chronically infected marmosets are described below.

Case 1: Cj05-002 (**Figures 1B** and **2**). The viral RNA was undetectable until week 4 post infection (p.i.) and then gradually increased to a peak at week 18 p.i. (3×10^7 copies/ml). Subsequently, this case retained intermittent viremia during the observation period of week 180 p.i., while the intervals between the viremia phases were prolonged. Importantly, the titers of anti-core and anti-NS3 antibodies reached a persistent plateau at 6 months and 1 year p.i., respectively. In addition, ALT levels were recurrently increased without observation of other clinical symptoms.

Case 2: Cj05-004 (**Figures 1B** and **2**). During the acute phase of infection, the level of viremia was relatively low and transient, followed by a 1-year period when the virus was essentially undetectable. Irrespective of the very low viral load, the titer of anti-NS3 but not anti-core antibody steadily increased and reached a plateau at week 42 p.i. Moreover, an occasional but obvious increase in the level of ALT was observed during this period. We thus suspected that antigenic stimulation by a lower level of viral growth in the liver, which remained below detectable levels in blood, might lead to the induction of the anti-NS3 antibody and the recurrent ALT increase. Subsequently, viremia became detectable at week 58 p.i. and 10^4–10^5 copies/ml of the viral RNA persisted until week 108 p.i. Thereafter, an abrupt increase of the anti-core antibody was detected, concomitant with augmentation of the viral load of $10^{5.5}$ copies/ml on average and recurrent increases in the ALT level. Eventually, the individual was euthanized at week 229 p.i. because of poor prognosis since the ALT value drastically increased by 161-fold, which was accompanied by a dramatic decrease of platelet counts and a deteriorating general status. Histopathological analyses of the necropsy samples demonstrated that the liver developed diffuse piecemeal necrosis with infiltration of lymphocytes and

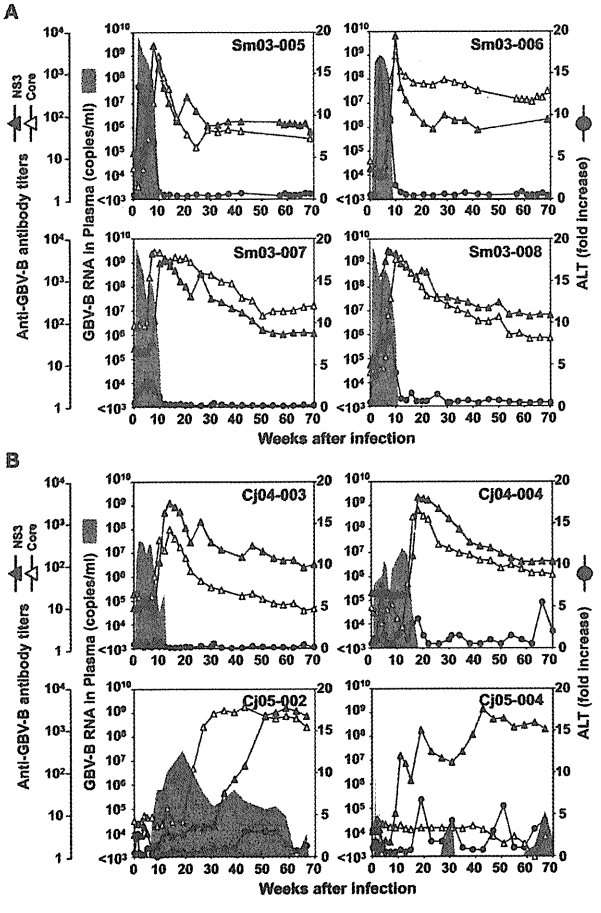

FIGURE 1 | Infection profiles until week 70 p.i. of tamarins (A) and marmosets (B) inoculated intrahepatically with GBV-B infectious serum obtained from a tamarin. Plasma samples periodically obtained from the monkeys were evaluated for the copy numbers of GBV-B genomic RNA (green shaded area), ALT levels (red circles), and the antibody titers against GBV-B core and NS3 (blue and yellow triangles, respectively).

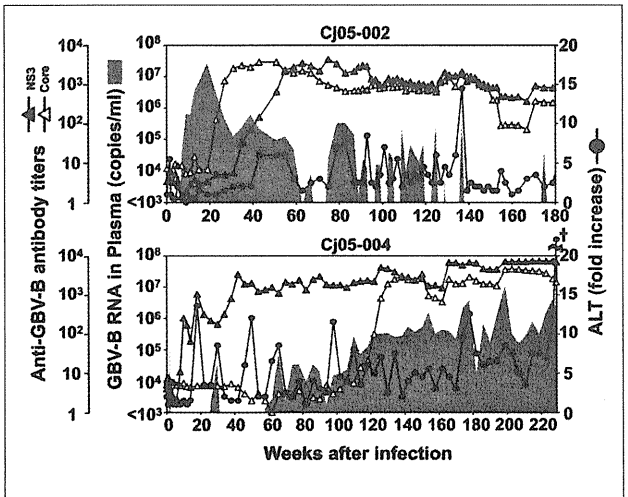

FIGURE 2 | Profiles of the marmosets persistently infected with GBV-B. Plasma samples periodically obtained from the marmosets were evaluated for the copy numbers of GBV-B genomic RNA (green shaded area), ALT levels (red circles), and the antibody titers against GBV-B core and NS3 (blue and yellow triangles, respectively). The cruciate mark in Cj05-004 indicates that the individual was euthanized due to a poor prognosis at week 229 p.i. At that time, the ALT value in plasma had increased by 161-fold.

formation of lymphoid follicles (**Figure 3A**, Appendix). The viral load in the liver was relatively high (3.8×10^4 copies/mg tissue weight), which was similar to the viral load observed for tamarins acutely infected with GBV-B (Ishii et al., 2007). The high viral load in the liver was consistent with a large number of granular positive signals for the core protein, which was in similar manner with the core protein of HCV (Miyanari et al., 2007), as immunostained with an anti-GBV-B core monoclonal antibody (**Figure 3B**). Notably, Masson trichrome staining (**Figures 3C,D**) as well as Elastica van Gieson staining (Appendix) demonstrated that the liver also developed diffuse and abundant fibrosis. The disease of this marmoset was therefore diagnosed as a case of acute exacerbation of progressive chronic hepatitis by GBV-B infection.

ANALYSIS OF MUTATIONS IN GBV-B GENOMES

Next, we determined the dominant sequence of the viral genomes at weeks 45, 104, and 135 p.i. in Cj05-002 and weeks 33, 88, 141, and 229 p.i. in Cj05-004. As seen in **Figure 4A**, it was found that there was no specific region in which extensive nucleotide mutations occurred throughout the study periods and that the nucleotide mutation rates were $1.9–2.9 \times 10^{-3}$ and $1.5–3.6 \times 10^{-3}$ changes per site per year in Cj05-002 and Cj05-004, respectively (**Table 1**). In terms of amino acid substitution, we observed the following: (i) several back or sequential mutations (G250V > A, S731L > S, E2346G > E in Cj05-002; V254A > V, I285V > I, L495S > L, T735A > T, F2135L > F > S in Cj05-004) in both marmosets; (ii) highly selective non-synonymous mutations that were remarkable in E1, but such mutations were rarely observed in core (**Figures 4** and **5**); and (iii) the non-synonymous mutation rates were $1.8–4.0 \times 10^{-3}$ and $2.1–4.6 \times 10^{-3}$ substitutions per site per year in Cj05-002 and Cj05-004, respectively (**Figures 4** and **5**; **Table 2**). (iv) The non-synonymous changes detected mainly in NS5A and NS5B in both animals were also observed in a number of previous reports (Simons et al., 1995; Bukh et al., 1999; Sbardellati et al., 2001; Martin et al., 2003; Nam et al., 2004; Kyuregyan et al., 2005; Weatherford et al., 2009; Takikawa et al., 2010). It may be reasonable to consider that the molecular clone we employed (Bukh et al., 1999) was derived from a minor clone of mixed populations and emergence of a new mutations easily occurred as a mechanism of GBV-B adaptation to a new host, while it is also possible that "consensus" non-synonymous changes were due to either a result of a selection of the pre-existent minor variants. Taken together, these results suggest that efficient

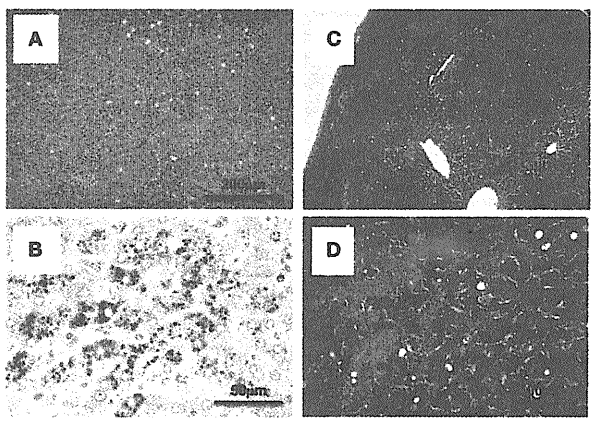

FIGURE 3 | Histopathological and immunohistochemical analyses of the liver from Cj05-004 at week 229 p.i. HE staining (A), immunohistochemical staining for the core protein of GBV-B (B), and Masson's trichrome staining (C,D) are shown.

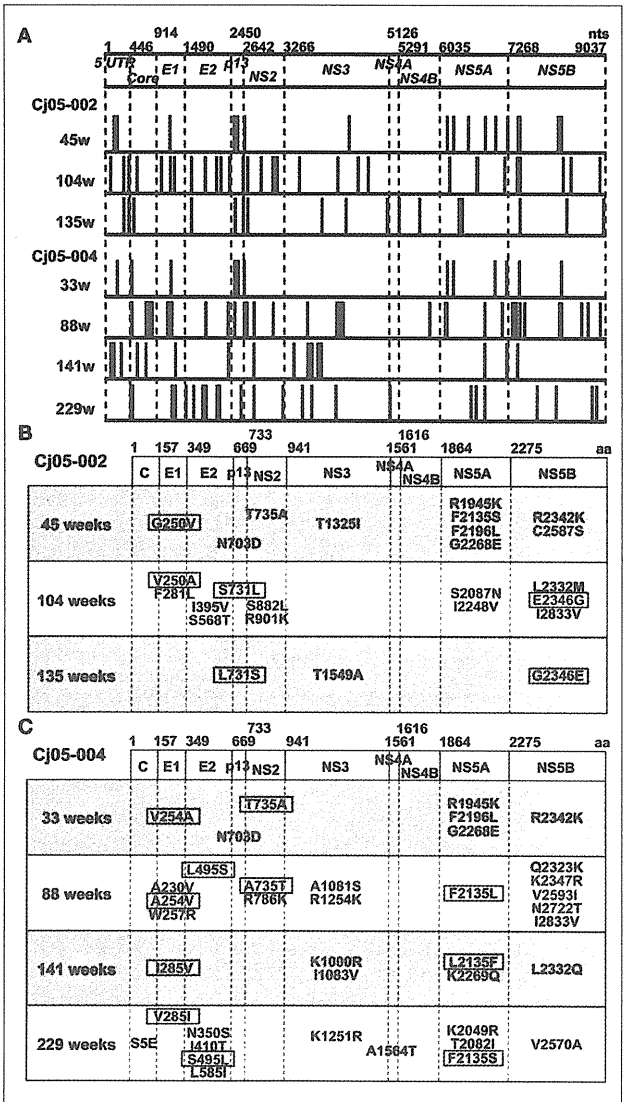

FIGURE 4 | Mutations in the viral genome sequences amplified from plasma of the marmosets persistently infected with GBV-B. (A) Positions of the nucleotide mutations in the viral genome sequences at multiple time points (at weeks 45, 104, and 135 in Cj05-002 and weeks 33, 88, 141, and 229 in Cj05-004) are illustrated as bars. **(B,C)** Positions of the non-synonymous mutations in the viral genome sequences at multiple time points are shown. **(B)** Cj05-002; **(C)** Cj05-004. Positions of the mutations that had been identified in previous reports are indicated as black, while those unidentified previously are shown as blue. Red squares illustrate back or sequential mutations.

Table 1 | Summary of the nucleotide substitutions in GBV-B genome sequences amplified from plasma of the marmosets persistently infected with GBV-B.

Genomic region	nt position	No. (%) of nt differences						
		Cj05-002			Cj05-004			
		45 weeks	104 weeks	135 weeks	33 weeks	88 weeks	141 weeks	229 weeks
5'UTR	1–445	2 (0.45)	3 (0.67)	2 (0.45)	1 (0.22)	0 (0)	3 (0.67)	0 (0)
Core	446–913	0 (0)	1 (0.21)	1 (0.21)	1 (0.21)	4 (0.85)	2 (0.43)	3 (0.64)
E1	914–1489	1 (0.17)	3 (0.52)	0 (0)	1 (0.17)	3 (0.52)	1 (0.17)	2 (0.35)
E2	1490–2449	0 (0)	5 (0.52)	1 (0.10)	0 (0)	2 (0.21)	1 (0.10)	6 (0.63)
p13	2450–2641	2 (1.04)	1 (0.52)	2 (1.04)	2 (1.04)	1 (0.52)	0 (0)	1 (0.52)
NS2	2642–3265	1 (0.16)	5 (0.80)	1 (0.16)	1 (0.16)	4 (0.64)	1 (0.16)	2 (0.32)
NS3	3266–5125	1 (0.05)	4 (0.22)	3 (0.16)	0 (0)	5 (0.27)	6 (0.32)	3 (0.16)
NS4A	5126–5290	0 (0)	0 (0)	0 (0)	0 (0)	0 (0)	0 (0)	1 (0.61)
NS4B	5291–6034	0 (0)	0 (0)	2 (0.27)	0 (0)	1 (0.13)	0 (0)	0 (0)
NS5A	6035–7267	6 (0.49)	4 (0.32)	2 (0.16)	4 (0.32)	4 (0.32)	2 (0.16)	3 (0.24)
NS5B	7268–9037	4 (0.23)	5 (0.28)	3 (0.17)	2 (0.11)	10 (0.56)	1 (0.06)	4 (0.23)
Total	9037	17 (0.19)	31 (0.34)	17 (0.19)	12 (0.13)	34 (0.38)	17 (0.19)	25 (0.28)
Mutation rate/year		2.2×10^{-3}	3.0×10^{-3}	3.2×10^{-3}	2.1×10^{-3}	3.6×10^{-3}	1.8×10^{-3}	1.6×10^{-3}

Table 2 | Summary of the amino acid substitutions in GBV-B genome sequences amplified from plasma of the marmosets persistently infected with GBV-B.

Amino acid region	aa position	No. (%) of aa differences						
		Cj05-002			Cj05-004			
		45 weeks	104 weeks	135 weeks	33 weeks	88 weeks	141 weeks	229 weeks
Core	1–156	0 (0)	0 (0)	0 (0)	0 (0)	0 (0)	0 (0)	1 (0.64)
E1	157–348	1 (0.52)	2 (1.04)	0 (0)	1 (0.52)	3 (1.56)	1 (0.52)	1 (0.52)
E2	349–613	0 (0)	2 (0.63)	0 (0)	0 (0)	1 (0.31)	0 (0)	4 (1.25)
P13	669–732	1 (1.56)	1 (1.56)	1 (1.56)	1 (1.56)	0 (0)	0 (0)	0 (0)
NS2	733–940	1 (0.48)	2 (0.96)	0 (0)	1 (0.48)	2 (0.96)	0 (0)	0 (0)
NS3	941–1560	1 (0.16)	0 (0)	1 (0.16)	0 (0)	2 (0.32)	2 (0.32)	1 (0.16)
NS4A	1561–1615	0 (0)	0 (0)	0 (0)	0 (0)	0 (0)	0 (0)	1 (1.82)
NS4B	1616–1863	0 (0)	0 (0)	0 (0)	0 (0)	0 (0)	0 (0)	0 (0)
NS5A	1864–2274	4 (0.97)	2 (0.49)	0 (0)	3 (0.73)	1 (0.24)	2 (0.49)	3 (0.73)
NS5B	2275–2864	2 (0.34)	3 (0.51)	1 (0.17)	1 (0.17)	5 (0.85)	1 (0.17)	1 (0.17)
Total	2864	10 (0.38)	12 (0.42)	3 (0.10)	7 (0.24)	14 (0.49)	6 (0.21)	12 (0.42)
Mutation rate/year		4.0×10^{-3}	3.7×10^{-3}	1.8×10^{-3}	3.9×10^{-3}	4.6×10^{-3}	2.1×10^{-3}	2.5×10^{-3}

and selective evasion from immune pressure in the two marmosets resulted in long-term persistent GBV-B infection accompanied by subsequent chronic hepatitis.

DISCUSSION

In this study, we show for the first time that GBV-B is capable of eliciting a chronic and progressive hepatitis C-like disease in marmosets. Evidence for this condition is demonstrated by long-term persistent GBV-B infection, recurrent ALT increase, and fibrosis. Moreover, one of the chronically infected marmosets developed acute exacerbation of chronic hepatitis as indicated by diffuse piecemeal liver necrosis and an ALT flare, which is seen in patients with viral hepatitis (Perrillo, 1997). While the usefulness of the monkey model as a surrogate model for HCV infection has been under debate due to the virtual inability of GBV-B to cause chronic hepatitis C-like disease in tamarins, the present data demonstrate that the ability of GBV-B to induce the chronic disease is likely to be inherent depending on the differences between species and individuals.

It has been reported that tamarins generally permit extensive replication of GBV-B in the subacute phase of infection and develop acute hepatitis as shown by significant increases of serum enzymes such as ALT and isocitrate dehydrogenase. The viral load in marmosets seems to be lower than in tamarins (Lanford et al.,

2003; Bright et al., 2004; Woollard et al., 2008; Weatherford et al., 2009). A recent report indicated that marmosets exhibit susceptible and partially resistant phenotypes upon infection with GBV-B (Weatherford et al., 2009). Consistent with this finding, the present results also showed that the marmosets appeared to exhibit two phenotypes (**Figure 1B**). Importantly, the long-term persistent GBV-B infection was established in the marmosets with lower viral loads during the initial weeks p.i. (**Figure 1B**; Cj05-002 and Cj05-004). This suggests that the mild viral growth in the marmosets with a "partially resistant" phenotype is critical for the establishment of the chronic infection. Of note, the viral growth was undetectable until week 6 p.i. in Cj05-002, owing to unexpected interferon responses that were induced by administration of an anti-luciferase small interfering RNA in a cationic liposome formulation 2 days before GBV-B infection (Yokota et al., 2007). Irrespective of the partial suppression of the viral growth, humoral immune responses were delayed and consequently the individual developed chronic infection. Taken together, it is reasonable to assume that the viral persistence in marmosets may be closely associated with inefficient antiviral immune responses that are elicited at the periods of the lower viral loads. Previously, we and others employed relatively higher amounts of GBV-B for challenge in tamarins and marmosets. This could result in greater viral loads in the acute phase than those in humans and chimpanzees infected with HCV, followed by induction of efficient protective immunity and acute clearance. To clarify the mechanisms by which chronic GBV-B infection is established, further characterization of the differences in innate and acquired antiviral immunity between individuals with acute clearance and chronic infection will be needed.

Accumulating evidence suggests that escape mutations occurring during the course of chronic HCV infection may lead to evasion of humoral and cellular antiviral immunity (Bowen and Walker, 2005a,b; Burke and Cox, 2010). Consistent with these observations, we found that GBV-B acquired multiple back or sequential non-synonymous mutations (e.g., G250V > A, S731L > S, E2346G > E in Cj05-002; and V254A > V, I285V > I, L495S > L, T735A > T, F2135L > F > S in Cj05-004) in the chronically infected marmosets. Highly selective non-synonymous mutations were identified especially in E1, but such mutations were rarely observed in core (**Figures 4** and **5**). Moreover, the non-synonymous mutations in the E1 and NS3 regions occurred throughout the observation periods in Cj05-004 with chronic GBV-B infection, which had not been identified previously (Simons et al., 1995; Bukh et al., 1999; Sbardellati et al., 2001; Martin et al., 2003; Nam et al., 2004; Kyuregyan et al., 2005; Weatherford et al., 2009; Takikawa et al., 2010). Together with the finding that the rates of both synonymous and non-synonymous mutations were similar to those observed in cases of HCV (Ogata et al., 1991; Fernandez et al., 2004), these results strongly suggest that efficient and selective evasion from immune pressures may result in long-term persistent GBV-B infection and subsequent chronic hepatitis. Further analyses on the functional significance of the non-synonymous mutations will clarify this possibility.

It is surprising that in Cj05-004, the antibody titer to NS3 was observed to steadily increase after week 10 p.i. irrespective of the scarce viral loads over 1 year p.i., including the bipartite

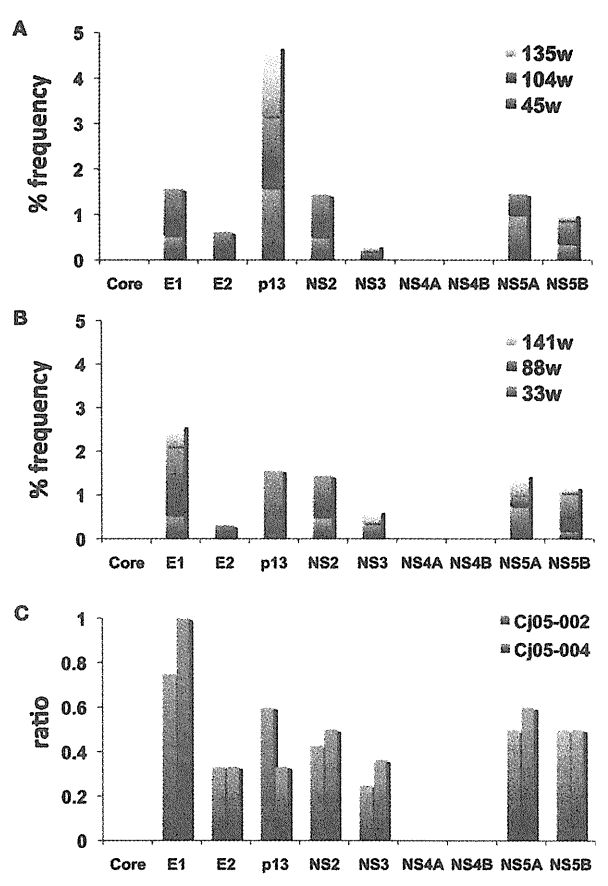

FIGURE 5 | The frequency of the non-synonymous mutations in the viral genome sequences amplified from plasma of the marmosets persistently infected with GBV-B. (A,B) The accumulated frequency of the non-synonymous mutations per total amino acid numbers of each viral protein at multiple time points are illustrated **[(A)** at weeks 45, 104, and 135 in Cj05-002; **(B)** weeks 33, 88, and 141 in Cj05-004]. To compare the frequency between the two marmosets, the data at week 229 p.i. in Cj05-004 are omitted. **(C)** The ratio of the non-synonymous mutations per total numbers of nucleotide mutations identified at weeks 45, 104, and 135 in Cj05-002 and at weeks 33, 88, and 141 in Cj05-004 in each viral gene. To compare the frequency between the two marmosets, the data at week 229 p.i. in Cj05-004 are omitted.

periods of weeks 4–26 and 34–58 p.i. when the virus was undetectable (**Figure 1**). Considering that three spikes of ALT levels were observed during these periods, our results suggest that antigenic stimulation by the lower level of viral growth in the liver, which was below detectable levels in blood, may induce the antibody and cytotoxic T-cell responses. In addition, during longitudinal analyses of monkeys experimentally infected with GBV-B, it is important to comprehensively evaluate multiple parameters, including viral loads, serum enzymes, and antibodies against core and NS3 proteins, to define whether virus-infected monkeys that produce no detectable viremia for a period of time have cleared the virus or are experiencing a latent period of chronic infection.

ACKNOWLEDGMENTS

We wish to thank T. Kurosawa, M. Fujita, and T. Ikoma for their helpful assistance and the members of Corporation for Production and Research of Laboratory Primates for technical assistance. Financial support: This work was supported by grants from the Ministry of Health, Labor, and Welfare of Japan (to Hirofumi Akari).

REFERENCES

Akari, H., Iwasaki, Y., Yoshida, T., and Iijima, S. (2009). Non-human primate surrogate model of hepatitis C virus infection. *Microbiol. Immunol.* 53, 53–57.

Beames, B., Chavez, D., Guerra, B., Notvall, L., Brasky, K. M., and Lanford, R. E. (2000). Development of a primary tamarin hepatocyte culture system for GB virus-B: a surrogate model for hepatitis C virus. *J. Virol.* 74, 11764–11772.

Beames, B., Chavez, D., and Lanford, R. E. (2001). GB virus B as a model for hepatitis C virus. *ILAR J.* 42, 152–160.

Boonstra, A., van der Laan, L. J., Vanwolleghem, T., and Janssen, H. L. (2009). Experimental models for hepatitis C viral infection. *Hepatology* 50, 1646–1655.

Bowen, D. G., and Walker, C. M. (2005a). Mutational escape from CD8+ T cell immunity: HCV evolution, from chimpanzees to man. *J. Exp. Med.* 201, 1709–1714.

Bowen, D. G., and Walker, C. M. (2005b). Adaptive immune responses in acute and chronic hepatitis C virus infection. *Nature* 436, 946–952.

Bright, H., Carroll, A. R., Watts, P. A., and Fenton, R. J. (2004). Development of a GB virus B marmoset model and its validation with a novel series of hepatitis C virus NS3 protease inhibitors. *J. Virol.* 78, 2062–2071.

Bukh, J. (2004). A critical role for chimpanzee model in the study of hepatitis C. *Hepatology* 39, 1469–1475.

Bukh, J., Apgar, C. L., and Yanagi, M. (1999). Toward a surrogate model for hepatitis C virus: An infectious molecular clone of the GB virus-B hepatitis agent. *Virology* 262, 470–478.

Bukh, J., Thimme, R., Meunier, J. C., Faulk, K., Spangenberg, H. C., Chang, K. M., Satterfield, W., Chisari, F. V., and Purcell, R. H. (2008). Previously infected chimpanzees are not consistently protected against reinfection or persistent infection after reexposure to the identical hepatitis C virus strain. *J. Virol.* 82, 8183–8195.

Burke, K. P., and Cox, A. L. (2010). Hepatitis C virus evasion of adaptive immune responses: a model for viral persistence. *Immunol. Res.* 47, 216–227.

Chisari, F. V. (2005). Unscrambling hepatitis C virus-host interactions. *Nature* 436, 930–932.

Feld, J. J., and Hoofnagle, J. H. (2005). Mechanism of action of interferon and ribavirin in treatment of hepatitis C. *Nature* 436, 967–972.

Fernandez, J., Taylor, D., Morhardt, D. R., Mihalik, K., Puig, M., Rice, C. M., Feinstone, S. M., and Major, M. E. (2004). Long-term persistence of infection in chimpanzees inoculated with an infectious hepatitis C virus clone is associated with a decrease in the viral amino acid substitution rate and low levels of heterogeneity. *J. Virol.* 78, 9782–9789.

Hoofnagle, J. H. (1997). Hepatitis C: the clinical spectrum of disease. *Hepatology* 26, 15S–20S.

Ishii, K., Iijima, S., Kimura, N., Lee, Y. J., Ageyama, N., Yagi, S., Yamaguchi, K., Maki, N., Mori, K., Yoshizaki, S, Machida, S., Suzuki, T., Iwata, N., Sata, T., Terao, K., Miyamura, T., and Akari, H. (2007). GBV-B as a pleiotropic virus: distribution of GBV-B in extrahepatic tissues in vivo. *Microbes Infect.* 9, 515–521.

Jacob, J. R., Lin, K. C., Tennant, B. C., and Mansfield, K. G. (2004). GB virus B infection of the common marmoset (*Callithrix jacchus*) and associated liver pathology. *J. Gen. Virol.* 85, 2525–2533.

Kyuregyan, K. K., Poleschuk, V. F., Zamyatina, N. A., Isaeva, O. V., Michailov, M. I., Ross, S., Bukh, J., Roggendorf, M., and Viazov, S. (2005). Acute GB virus B infection of marmosets is accompanied by mutations in the NS5A protein. *Virus Res.* 114, 154–157.

Lanford, R. E., Chavez, D., Notvall, L., and Brasky, K. M. (2003). Comparison of tamarins and marmosets as hosts for GBV-B infections and the effect of immunosuppression on duration of viremia. *Virology* 311, 72–80.

Lavanchy, D. (2009). The global burden of hepatitis C. *Liver Int.* 29, 74–81.

Martin, A., Bodola, F., Sanger, D. V., Goettge, K., Popov, V., Rijnbrand, R., Lanford, R. E., and Lemon, S. M. (2003). Chronic hepatitis associated with GB virus B persistence in a tamarin after intrahepatic inoculation of synthetic viral RNA. *Proc. Natl. Acad. Sci. U.S.A.* 100, 9962–9967.

Melnikova, I. (2008). Hepatitis C therapies. *Nat. Rev. Immunol.* 5, 799–800.

Miyanari, Y., Atsuzawa, K., Usuda, N., Watashi, K., Hishiki, T., Zayas, M., Bartenschlager, R., Wakita, T., Hijikata, M., and Shimotohno, K. (2007). The lipid droplet is an important organelle for hepatitis C virus production. *Nat. Cell Biol.* 9, 1089–1097.

Muerhoff, A. S., Leary, T. P., Simons, J. N., Pilot-Matias, T. J., Dawason, G. J., Erker, J. C., Chalmers, M. L., Schlauder, G. G., Desai, S. M., and Mushahwer, I. K. (1995). Genomic organization of GB viruses A and B: two new members of the Flaviviridae associated with GB agent hepatitis. *J. Virol.* 69, 5621–5630.

Nam, J. H., Faulk, K., Engle, R. E., Govindarajan, S., St. Claire, M., and Bukh, J. (2004). In vivo analysis of the 3′ untranslated region of GB virus B after in vitro mutagenesis of an infections cDNA clone: persistent infection in a transfected tamarin. *J. Virol.* 78, 9389–9399.

Ogata, N., Alter, H. J., Miller, R. H., and Purcell, R. H. (1991). Nucleotide sequence and mutation rate of the H strain of hepatitis C virus. *Proc. Natl. Acad. Sci. U.S.A.* 88, 3392–3396.

Ohba, K., Mizokami, M., Lau, J. Y., Orito, E., Ikeo, K., and Gojobori, T. (1996). Evolutionary relationship of hepatitis C, pesti-, flavi-, plantviruses, and newly discovered GB hepatitis agents. *FEBS Lett.* 378, 232–234.

Perrillo, R. P. (1997). The role of liver biopsy in hepatitis C. *Hepatology* 26, 57S–61S.

Rehermann, B., and Nascimbeni, M. (2005). Immunology of hepatitis B virus and hepatitis C virus infection. *Nat. Rev. Immunol.* 5, 215–229.

Sbardellati, A., Scarselli, E., Verschoor, E., De Tomassi, A., Lazzaro, D., and Traboni, C. (2001). Generation of infectious and transmissible virions from a GB virus B full-length consensus clone in tamarins. *J. Gen. Virol.* 82, 2437–2448.

Seeff, L. B., and Hoofnagle, J. H. (2002). National Institutes of Health Consensus Development Conference: management of hepatitis C: 2002. *Hepatology* 36, S1–S2.

Simons, J. N., Pilot-Matias, T. J., Leary, T. P., Dawason, G. J., Desai, S. M., Schlauder, G. G., Muerhoff, A. S., Erker, J. C., Buijk, S. L., Chalmers, M. L., Van Sant, C. L., and Mushahwar, I. K. (1995). Identification of two *Flavivirus*-like genomes in the GB hepatitis agent. *Proc. Natl. Acad. Sci. U.S.A.* 92, 3401–3405.

Takikawa, S., Engle, R. E., Faulk, K. N., Emerson, S. U., Purcell, R. H., and Bukh, J. (2010). Molecular evolution of GB virus B hepatitis virus during acute resolving and persistent infections in experimentally infected tamarins. *J. Gen. Virol.* 91, 727–733.

Weatherford, T., Chavez, D., Brasky, K. M., and Lanford, R. E. (2009). The marmoset model of GB virus B infections: adaptation to host phenotypic variation. *J. Virol.* 83, 5806–5814.

Woollard, D. J., Haqshenas, G., Dong, X., Pratt, B. F., Kent, S. J., and Gowans, E. J. (2008). Virus-specific T-cell immunity correlates with control of GB virus B infection in marmosets. *J. Virol.* 82, 3054–3060.

Yokota, T., Iijima, S., Kubodera, T., Ishii, K., Katakai, Y., Ageyama, N., Chen, Y., Lee, Y. J., Unno, T., Nishina, K., Iwasaki, Y., Maki, N., Mizusawa, H., and Akari, H. (2007). Efficient regulation of viral replication by siRNA in a non-human primate surrogate model for hepatitis C. *Biochem. Biophys. Res. Commun.* 361, 294–300.

Conflict of Interest Statement: The authors declare that the research was conducted in the absence of any commercial or financial relationships that could be construed as a potential conflict of interest.

Received: 21 October 2011; paper pending published: 31 October 2011; accepted: 15 November 2011; published online: 07 December 2011.

Citation: Iwasaki Y, Mori K-i, Ishii K, Maki N, Iijima S, Yoshida T, Okabayashi S, Katakai Y, Lee Y-J, Saito A, Fukai H, Kimura N, Ageyama N, Yoshizaki S, Suzuki T, Yasutomi Y, Miyamura T, Kannagi M and Akari H (2011) Long-term persistent GBV-B infection and development of a chronic and progressive hepatitis C-like disease in marmosets. Front. Microbio. 2:240. doi: 10.3389/fmicb.2011.00240

This article was submitted to Frontiers in Virology, a specialty of Frontiers in Microbiology.

APPENDIX

MATERIALS AND METHODS

Liver samples obtained by necropsy from the GBV-B-infected marmosets were histopathologically analyzed as described in Section "Materials and Methods." Elastica–van Gieson staining was performed to evaluate fibrosis according to a standard laboratory protocol. To detect CD3 and CD20 antigens, liver samples were fixed in 10% neutral buffered formalin and embedded in paraffin wax. Sections were deparaffinized by pretreatment with 0.5% periodic acid and then subjected to antigen retrieval with citric acid buffer and heating in an autoclave for 10 min at 121°C. Sections were then incubated free floating in the monoclonal antibody solution for CD20 (DAKO) and CD3 (DAKO) overnight at 4°C. Following brief washes with buffer, the sections were sequentially incubated with biotinylated goat anti-mouse IgG (1:400), followed by streptavidin–biotin–horseradish peroxidase complex (sABC kit; DAKO, Denmark). Immunoreactive elements were visualized by treating the sections with 3,3′-diaminobenzidine tetroxide (Dojin Kagaku, Japan). The sections were then counterstained with hematoxylin.

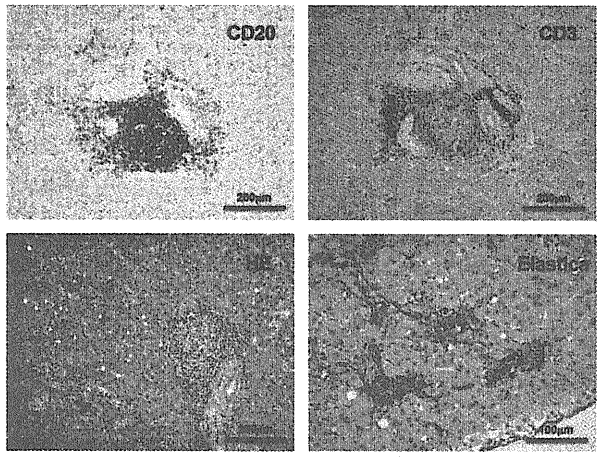

FIGURE A1 | Histopathological and immunohistochemical analyses of the liver from Cj05-004 at week 229 p.i.

Virology 421 (2011) 96–104

Contents lists available at SciVerse ScienceDirect

Virology

journal homepage: www.elsevier.com/locate/yviro

Analyses of mutations selected by passaging a chimeric flavivirus identify mutations that alter infectivity and reveal an interaction between the structural proteins and the nonstructural glycoprotein NS1

Evandro R. Winkelmann [a], Douglas G. Widman [b,d], Ryosuke Suzuki [a,e], Peter W. Mason [a,b,c,f,*]

[a] Department of Pathology, University of Texas Medical Branch, Galveston, TX 77555-0436, USA
[b] Department of Microbiology and Immunology, University of Texas Medical Branch, Galveston, TX 77555-0436, USA
[c] Sealy Center for Vaccine Development, University of Texas Medical Branch, Galveston, TX 77555-0436, USA
[d] Lineberger Comprehensive Cancer Center, University of North Carolina, Chapel Hill, NC 27599-7295, USA
[e] National Institute of Infectious Diseases, Shinjuku-ku, Tokyo 162-8640, Japan
[f] Microbial Molecular Biology, Novartis Vaccines and Diagnostics, Cambridge, MA, 02139, USA

ARTICLE INFO

Article history:
Received 6 May 2011
Returned to author for revision 6 June 2011
Accepted 8 September 2011
Available online 13 October 2011

Keywords:
Flavivirus
Single-cycle virus
Chimera
RepliVAX
Packaging

ABSTRACT

We previously described a single-cycle dengue vaccine (RepliVAX D2) engineered from a capsid (C) gene-deleted West Nile virus (WNV) expressing dengue virus serotype 2 (DENV2) prM/E genes in place of the corresponding WNV genes. That work demonstrated that adaptation of RepliVAX D2 to grow in WNV C-expressing cells resulted in acquisition of non-synonymous mutations in the DENV2 prM/E and WNV NS2A/NS3 genes. Here we demonstrate that the prM/E mutations increase the specific infectivity of chimeric virions and the NS2A/NS3 mutations independently enhance packaging. Studies with the NS2A mutant demonstrated that it was unable to produce a larger form of NS1 (NS1'), suggesting that the mutation had been selected to eliminate a ribosomal frame-shift "slippage site" in NS2A. Evaluation of a synonymous mutation at this slippage site confirmed that genomes that failed to make NS1' were packaged more efficiently than WT genomes supporting a role for NS1/NS1' in orchestrating virion assembly.

Introduction

Flaviviruses are single-stranded, positive-sense RNA viruses and have an 11-kb genome with a single open reading frame encoding three structural proteins (C, prM/M and E) and seven non-structural proteins (NS1, NS2A, NS2B, NS3, NS4A, NS4B and NS5). Flavivirus RNA replication occurs in the cell cytoplasm via a negative-strand RNA intermediate, ultimately leading to the accumulation of positive-strand RNAs. Several NS proteins have been implicated in genome replication. The NS2B/NS3 serine protease is required for proteolytic processing at multiple sites in the viral polyprotein. NS3 also possesses RNA triphosphatase and RNA helicase activities and NS5 contains methyltransferase and RNA-dependent RNA polymerase activities (Lindenbach et al., 2007). NS1 is a non-structural glycoprotein that is secreted from mammalian but not insect cells infected by flaviviruses (Mason, 1989), and is found at high concentrations in the blood of viremic dengue patients (Alcon et al., 2002; Libraty et al., 2002).

NS1 is found in the viral polyprotein immediately following the two structural proteins, prM/E. The coding regions of these proteins are separated by signal peptidase cleavage sites, and all three proteins acquire N-linked carbohydrates during their synthesis (Lindenbach et al., 2007). prM and E form heterodimers which eventually undergo a complicated maturation process that produces E dimers that cover the surface of the mature viral particle (Li et al., 2008; Yu et al., 2008). Early studies demonstrated that NS1 was slowly secreted from mammalian cells, and studies with trans-expressed prM/E/NS1 cassettes suggested a role for NS1 in virion morphogenesis (Fan and Mason, 1990; Konishi et al., 1991; Mason, 1989). However, work with NS1 mutants demonstrated that NS1 played an essential role in viral RNA replication (Muylaert et al., 1996; Muylaert et al., 1997).

The insect-vectored flaviviruses are responsible for considerable morbidity and mortality worldwide. The viruses exist on all continents of the world except Antarctica, and threaten much of the world's population. DENV infections are estimated to occur in up to 100 million individuals annually and over 2.5 billion people live in areas at risk for DENV infection. Vaccines are available for a number of flavivirus diseases, including YF and JE, but there are currently no vaccines available for dengue. Among the marketed vaccines, the YF vaccine, which consists of the live-attenuated strain YF-17D, has been widely recommended to travelers, and has been considered to be remarkably safe and efficacious. However, recent documentation

* Corresponding author at: Novartis Vaccines and Diagnostics, Inc., 45 Sidney Street, Cambridge, MA 02139, USA.
E-mail address: peter.mason@novartis.com (P.W. Mason).

0042-6822/$ – see front matter © 2011 Elsevier Inc. All rights reserved.
doi:10.1016/j.virol.2011.09.007

of disease in a tiny fraction of those vaccinated with YF-17D prompted reconsideration of its safety and as a result, the American Committee on Immunization Practices now recommends that the risk of infection with YFV be taken into account when vaccinating travelers from non-endemic regions (Staples et al., 2010). Nevertheless, YF-17D continues to be an important public health tool, and has undisputable benefit in populations at high risk of YFV infection. In the case of JE vaccines, a live-attenuated vaccine is widely used in China, but safety and manufacturing issues have restricted it from being used in other regions of the world (Halstead and Thomas, 2011). In these areas, the product of choice was an efficacious inactivated mouse-brain derived virus, but safety concerns prompted its removal from use. However, new products, including cell-culture derived inactivated vaccines and a chimeric live-attenuated product based on YFV 17D are now being marketed in developed economies (Halstead and Thomas, 2011).

Recently, we reported the development of single-cycle flaviviruses that can be used as safe and effective vaccines (Mason et al., 2006). This single-cycle technology has been used to produce a series of vaccine candidates (named RepliVAX), that encode genomes harboring a truncated C (trC) gene that prevents the RepliVAX genome from being packaged into infectious particles unless the C gene is supplied in *trans* (Ishikawa et al., 2008; Mason et al., 2006; Suzuki et al., 2009; Widman et al., 2008). RepliVAX can infect normal cells in vaccinated animals, and these infected cells release prM/E-containing sub-viral particles (SVPs) and NS1 that induce effective antiviral immune responses. However, RepliVAX cannot spread or cause disease in animals, thus making them safe live-attenuated vaccines. The most recent addition to the RepliVAX family is a chimeric RepliVAX that expresses the prM/E genes of DENV2 in place of the WNV structural genes, and this vaccine (RepliVAX D2) was able to control DENV2 disease in a mouse model for DENV2 infection (Suzuki et al., 2009).

During our development of RepliVAX D2, we discovered that the initial construct grew poorly in C-expressing cells, but that growth could be improved by extensive blind passage (facilitated by introduction of larger fragments of the C gene and passaging of packaging cells along with the single-cycle virus). Analyses of these blind-passaged variants demonstrated that their improved growth characteristics were associated with the acquisition of specific mutations in the coding regions for prM, E, NS2A and NS3. In the case of the mutations in prM and E, we used reverse genetics to show that a pair of mutations in M (amino acid 9: G->R and amino acid 13: E->V; referred to by convention as $M^{R9G,V13E}$) and a single mutation in E (E^{K120T}; numbering convention as shown for M) both operated individually to increase yield of RepliVAX D2 in culture, but the combination of the M and E mutations worked together to produce the greatest enhancement in viral growth (Suzuki et al., 2009). Further, we showed that the mutations in the NS2A ($NS2A^{S9F}$) and the NS3 genes of the WNV backbone ($NS3^{R516K}$) enhanced growth of a re-engineered RepliVAX D2, but did not appear to have an effect on genome replication *per se*, since they were unable to enhance replication of WNV replicons that did not contain DENV genes (Suzuki et al., 2009).

Here we report that the mutations we identified in the growth-adapted chimeric RepliVAX D2 constructs in the DENV2 prM and E region improve specific infectivity of flavivirus particles in a manner similar to that of a previously characterized heparan sulfate (HS)-binding mutation at a nearby position in E (E^{K126E}) (Lee et al., 2006). In addition, we demonstrate that the mutation in the WNV NS2A (which acts in concert with the WNV NS3 mutation) eliminates the production of an altered form of NS1 (NS1') that arises from ribosome slippage at a site found in WNV, but not DENV (Firth and Atkins, 2009; Melian et al., 2010). Finally, we demonstrate that the elimination of the production of NS1' by introduction of a synonymous mutation in this ribosomal slippage site improved encapsidation of particles without altering the amplification and translation of the genome, indicating a functional interaction between NS1/NS1' and the structural proteins of flaviviruses during encapsidation.

Results

Mutations in DENV prM/E increase growth and alter specific infectivity

To determine how growth-enhancing mutations in the DENV2 prM/E coding region of single-cycle chimeric flaviviruses expressing the prM/E genes of DENV2 and the NS genes of WNV function (Suzuki et al., 2009), we produced a series of packaging cell lines (see Fig. 1A) that encoded the low passage DENV2 New Guinea C (NGC) prM/E sequences [BHK(VEErep/WNVC*-DENV2prM/E/Pac)] used to make our first generation RepliVAX D2 as well as a cell line [BHK(VEErep/WNVC*-DENV2pr/$M^{R9G,V13E}$/E^{K120T}/Pac)] that encoded the DENV2 prM/E sequences selected when RepliVAX D2 was adapted to grow in cells expressing the C gene (Suzuki et al., 2009). These packaging cells, along with cell lines carrying packaging constructs expressing the WNV prM/E [BHK(VEErep/WNVC*-E/Pac)], the JEV prM/E [BHK (VEErep/WNVC*-JEVprM/E/Pac)], and a cell line [BHK(pVEErep/WNVC*-DENV2prM/E^{K126E}/Pac] expressing an E protein from a high-passage NGC strain of DENV that contains a DENV2 E mutation (E^{K126E}) previously associated with HS binding (Lee et al., 2006) (see Fig. 1A) were used to produce viral replicon particles (VRPs) containing a WNV replicon (C-hFLuc2A-NS1-5, see Fig. 3A). When these VRPs, which contained identical WNV-derived replicons transpackaged in the different coats provided by their packaging cell lines (Fig. 1A), were tested side-by-side for their specific infectivities in Vero cells (genome copies per IU; see Materials and methods), we discovered that the VRPs packaged in WNV or JEV prM/E proteins exhibited significantly better specific infectivities (500 to 2000 genome copies per IU) than particles packaged in any of the DENV2 coats (50,000 to 200,000 genome copies per IU; Fig. 1B). Among the DENV2-packaged VRPs, the VRPs coated with the prM/E proteins of a low-passage NGC strain [from BHK(VEErep/WNVC*-DENV2prM/E/Pac)] displayed the poorest infectivity (over 200,000 genome equivalents per IU), and the particles packaged in coats containing the previously identified HS-binding mutation at position 126 (Lee et al., 2006) [BHK(pVEErep/WNVC*-DENV2prM/E^{K126E}/Pac)] displayed a slightly better specific infectivity. Interestingly, the VRPs packaged in the cell lines encoding the DENV2 prM/E genes selected in our RepliVAX D2 passaging studies (Suzuki et al., 2009) [BHK(VEErep/WNVC*-DENV2pr/$M^{R9G,V13E}$/E^{K120T}/Pac)] displayed a significantly better specific infectivity than the particles packaged in the WT DENV2-packaged VRPs, which contained the same low-passage DENV2 genes used to initiate the passaging studies we performed with RepliVAX D2 (Suzuki et al., 2009) (Fig. 1B). Taken together, these data demonstrate that the previously reported low-specific infectivity of DENV particles (van der Schaar et al., 2007) is due to the properties of the virion surface proteins and that changes in specific infectivity in cell culture can be facilitated by addition of positively charged residues in M and E that presumably function by facilitating productive binding of negatively charged glycosaminoglycans (GAGs) such as HS that are ubiquitously expressed on cells in culture and aid in infection as previously demonstrated for DENV2 (Lee et al., 2006). However, we cannot rule out the possibility that the mutations in prM/E could also have a role in the maturation of the structural proteins needed for flavivirus morphogenesis, especially in light of recent work showing that extracellular DENV particles contain a mixture of mature (lacking prM) and immature particles (Junjhon et al., 2010) which likely contribute to their poor specific infectivity.

NS2A and NS3 mutations previously selected in DENV2/WNV chimeras improve VRP growth when packaged in DENV2 envelopes

During propagation of a derivative of RepliVAX D2 containing the prM/E mutations described above (Suzuki et al., 2009), two mutations were selected in the WNV nonstructural protein-encoding regions that improved the growth of these chimeric viruses. To help learn how these mutations exerted their effects, we introduced

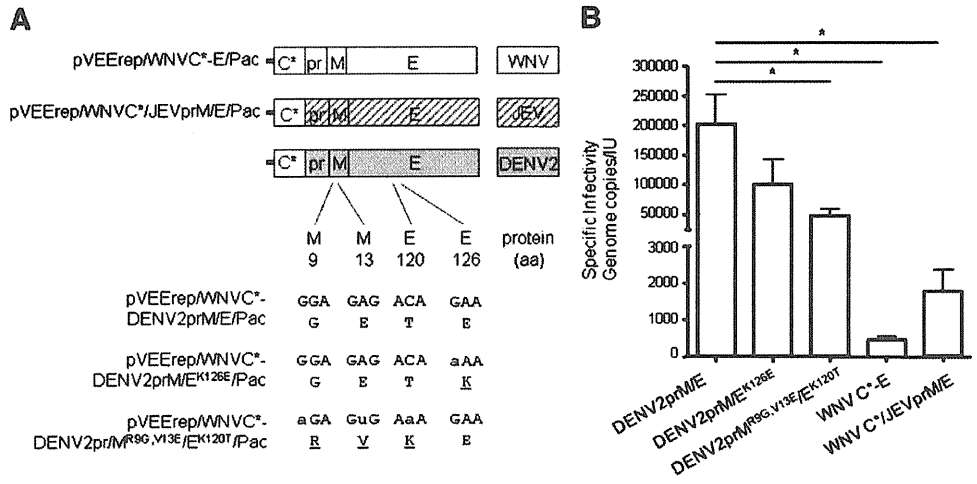

Fig. 1. Effect of flavivirus M/E proteins on the specific infectivity of trans-encapsidated WNV replicon genomes. (A) Schematic representation of the packaging cell constructs. All constructs contained a form of the WNV C protein (C*) engineered to contain synonymous mutations in the start of the genome to prevent generation of homologous recombinants with the replicons, as well as complete prM/E cassettes from the indicated viruses (see Materials and methods); "aa" indicates the position of the affected codon within the individual protein-coding regions. (B). Specific infectivities of VRPs created by packaging a WNV-derived replicon [pWNR C-hFLuc2A NS1-5-encoding hFLuc (see Materials and methods and Fig. 3A)]. Data displayed indicate the particle number (determined by genome quantification using sqPCR) divided by the measured infectivity on Vero cells (see Materials and methods). Error bars indicate the standard deviation between specific infectivity determinations established from two measurements of RNA concentration from the linear range of the sqPCR standard curve. "*" denotes significance as measured by one-way ANOVA with Bonferroni post-test ($p<0.05$).

them into RepliVAX WN (as single or double mutations; Fig. 2A), and tested how these mutations affected the growth of this non-chimeric single-cycle virus in a WNV C-expressing cell line [BHK(VEErep/Pac-Ubi-C*)]. Fig. 2B shows growth curves for the WT and mutated RepliVAX WN that were created by averaging values from 3 independent experiments. These growth curves demonstrate that the mutations selected in the context of the chimeric RepliVAX D2 were unable to produce a detectable improvement in growth of the non-chimeric RepliVAX WN.

To further evaluate the interactions between WNV NS2A and NS3 mutations and the DENV2 prM/E cassettes, NS2A^{S9F} and NS3^{R516K} were introduced as single- or double-mutations into a WNV replicon encoding a humanized form of the firefly luciferase (hFLuc) reporter gene (Fig. 3A). Comparison of the ability of VRPs containing these replicons to grow in a subset of the packaging cells described in Fig. 1 demonstrated that each of the non-structural protein mutations enhanced growth in all three of the DENV2 packaging cell lines (Figs. 3B, C and D). In addition, the two mutations displayed an additive/synergistic effect on transpackaging within DENV2 envelopes (Figs. 3B, C and D). However, neither of these mutations (independently or together) produced a detectable improvement in the growth of this WNV-derived replicon when replicons carrying these mutations were propagated in packaging cells expressing the WNV envelope protein cassette (Fig. 3E).

NS2A^{S9F} mutation alters the production of a higher molecular weight form of NS1

The recent observation that the NS2A gene of encephalitic flaviviruses contains a frame-shift motif (Firth and Atkins, 2009) that permits the production of an altered form of NS1 [known as NS1'; (Melian et al., 2010)] identified over 20 years ago in cells infected with JEV (Mason, 1989) prompted us to further examine our NS2A^{S9F} mutation. Interestingly, this mutation disrupts the canonical UUUU portion of the ribosome slip site that produces NS1' (CCCUUUU->CCCUUcU; Fig. 4A). To confirm that this mutation prevented the synthesis of NS1', we conducted Western blot analyses, that clearly demonstrate that this mutation results in the loss of NS1' (Fig. 4B).

Mutation of the ribosome slip site in NS2A enhances packaging of WN replicons in DENV2 coats and eliminates production of NS1'

To demonstrate that the growth enhancing properties of the NS2A^{S9F} mutation resulted through the abrogation of NS1' production, we engineered two silent mutations (CCCUUUU->CCC cUUc) in this region of NS2A (producing a construct designated NS2A^{F9F}) that disrupted the ribosome slip site (Fig. 5A). WNV replicons bearing this mutation alone, or in the presence of the NS3 mutation, displayed a significant enhancement of growth compared to the WT replicon genome when they were grown in cell lines providing DENV2 coats (Figs. 5B, C and D). Furthermore, Fig. 5E shows that the NS2A^{F9F} mutation, alone, or in concert with the NS3^{R516K} mutation produced a significant improvement in packaging in a WNV coat at several time points. As expected from the intentional disruption of the slippage site, cells infected with replicons expressing the NS2A^{F9F} mutation alone, or in the presence of the NS3^{R516K} mutation did not produce any detectable NS1' (Fig. 5F). To further understand the interaction between the NS2A^{F9F}and NS3^{R516K} mutations and DENV coats, we investigated the specific infectivity of C-hFLuc2A-NS1-5 and C-hFLuc2A-NS1-5 NS2A^{F9F} NS3^{R516K} VRPs produced in the WNVC*-DENV2pr/M^{R9G,V13E}/E^{K120T} and the WNVC*-E cell lines harvested from the 72 hpi time point in the study shown in Figs. 5D and E. These studies showed improved infectivity for the DENV-packaged VRPs that carried the NS2A frame-shift and NS3 mutations relative to the WT genomes, but no difference in the infectivity of the WNV-packaged genomes containing these mutations (Figs. S2A and B), suggesting that the C-hFLuc2A-NS1-5 NS2A^{F9F} NS3^{R516K} were more efficiently assembled into infectious DENV particles. Furthermore, Western blot analyses of the E protein content of these same VRP preparations showed a similar level of incorporation of WNV E into VRPs produced with either mutant or WT NS genes, but a more efficient incorporation of the DENV E into particles carrying the mutant NS genes, consistent with the hypothesis that the NS2A frame-shift and NS3 mutations produced higher infectious yields by increasing efficiency of assembly of infectious particles with DENV coats.

To further evaluate the role of these mutations in virion packaging in WNV coats, we utilized an additional, more sensitive assay consisting of calculating the size of infectious foci formed by VRPs carrying WT and mutant replicons on BHK(VEErep/WNVC*-E/Pac) cells.

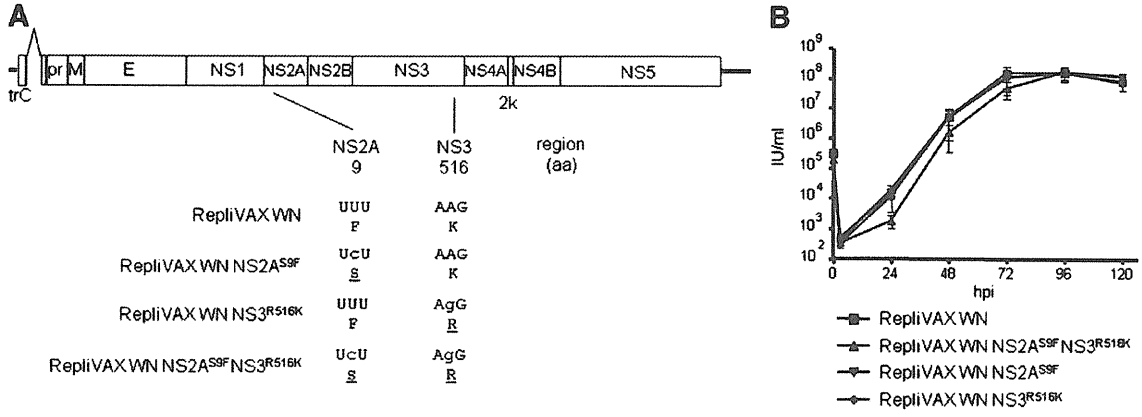

Fig. 2. NS2A^{S9F} and NS3^{R516K} mutations do not significantly improve the growth of RepliVAX derivatives carrying the WNV prM/E genes. (A) Schematic representation of derivatives of RepliVAX WN carrying mutations in NS2A and NS3; "aa" indicates the position of the affected codon within the individual protein-coding regions. (B) Growth curves of the RepliVAX WN constructs shown in Fig. 2A on BHK(VEErep/Pac-Ubi-C*) which express the WNV C protein. Cells were infected at an MOI of 0.01, and media were harvested, and titered at the indicated time points as described in the Materials and methods. The first time point (0 hpi) indicates the initial dose used to infect the cells. Values represent averages of three individual experiments. Error bars indicate standard deviation.

Fig. 6 shows the results of these assays, which support the data in Fig. 5E, by showing that all three VRPs tested in these assays tended to produce larger foci on cells expressing the WNV structural proteins.

NS1 is required for flavivirus genome replication, and mutations in NS1 have been shown to alter genome replication in cells in culture (see Introduction). To determine if the effect of NS1' abrogation was producing the enhanced growth/spread phenotype in packaging cell lines, we infected WT BHK cells with VRPs harboring various replicons and used the short-lived hFLuc reporter gene (Thompson et al., 1991) to quantify the levels of their genome replication and polyprotein translation. These studies, shown in Fig. 7, showed that neither the NS2A^{F9F}, NS3^{R516K}, nor the combined NS2A^{F9F}/NS3^{R516K} mutations significantly altered the levels of replicon amplification at 24 h post infection.

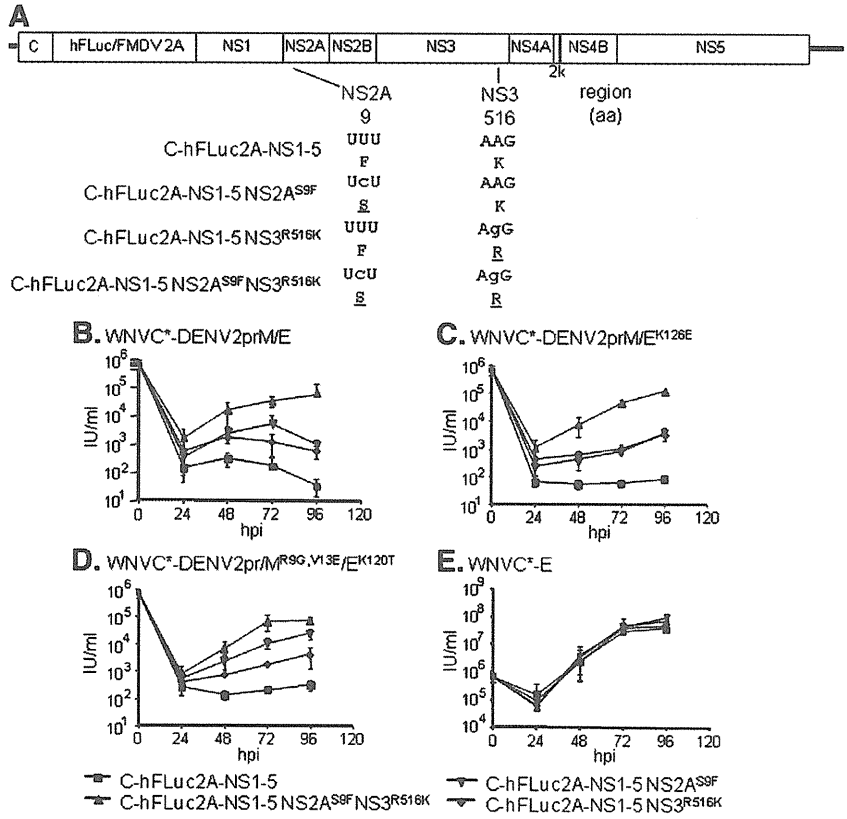

Fig. 3. NS2A^{S9F} and NS3^{R516K} improve growth of WNV VRPs when transpackaged in DENV coats. (A) Schematic representation of derivatives of WNV replicons carrying mutations in NS2A and NS3; "aa" indicates the position of the affected codon within the individual protein-coding regions. (B–E) Growth curves of VRPs harboring the genomes shown in Fig. 3A on BHK cell lines encoding the indicated packaging constructs. Cell monolayers were infected at an MOI of 0.05 with the indicated VRPs, and media were harvested and titered at the indicated time points as described in the Materials and methods. The first time point (0 hpi) indicates the initial dose used to infect the cells. Values represent averages of two individual experiments. Error bars indicate standard deviation.

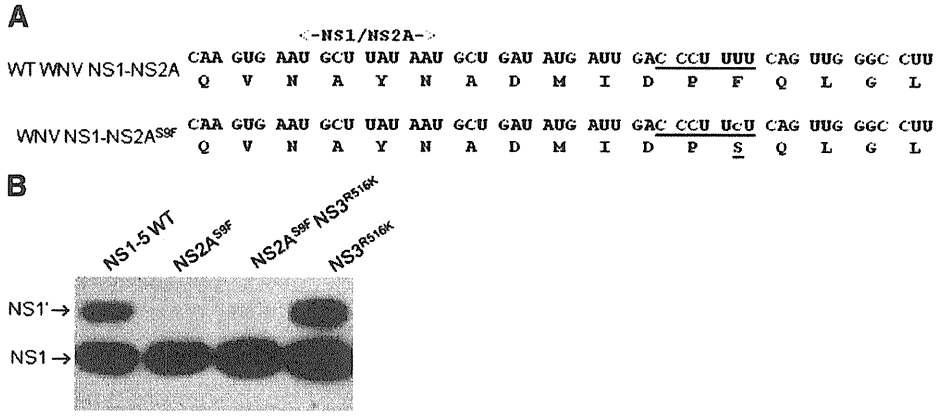

Fig. 4. Effect of NS2A^{S9F} mutation on synthesis of NS1'. (A) Alignment of RNA and amino acid sequences at the NS1/NS2A junction region of WNV showing the ribosomal frame-shift site (underlined) and its disruption by the NS2A^{S9F} mutation. (B) Western blot showing that cells infected with replicons encoding the NS2A^{S9F} mutation fail to produce NS1'. Cells infected with particles encoding C-hFLuc2A-NS1-5 replicon (labeled NS1-5 WT) and its derivatives (see Fig. 3A; labeled in this panel by mutation only) were lysed, blotted, and immunostained as described in the Materials and methods.

Discussion

Flaviviruses display a broad host- and cell-specificity which suggests that these viruses can use a variety of cell surface receptors. Multiple molecules have been identified that can serve as receptors, but the most clearly documented example of a cell-surface component that can be utilized as a receptor is the GAG, HS. Although the role of HS in natural infections by RNA viruses remains unclear, flaviviruses that are adapted to grow in cell culture or in specific animal models can acquire the ability to bind to HS through the acquisition of mutations on the E protein that produce positively charged patches that efficiently bind negatively charged GAGs (Anez et al., 2009; Kroschewski et al., 2003; Lee et al., 2004; Lee and Lobigs, 2000; Lee and Lobigs, 2002; Lee et al., 2006; Mandl et al., 2000). In the current studies we used a transpackaging system to demonstrate that the DENV2 M/E protein mutations found in our previously reported cell-adapted dengue chimera (Suzuki et al., 2009) improve the specific infectivity of transpackaged particles, explaining the selection of

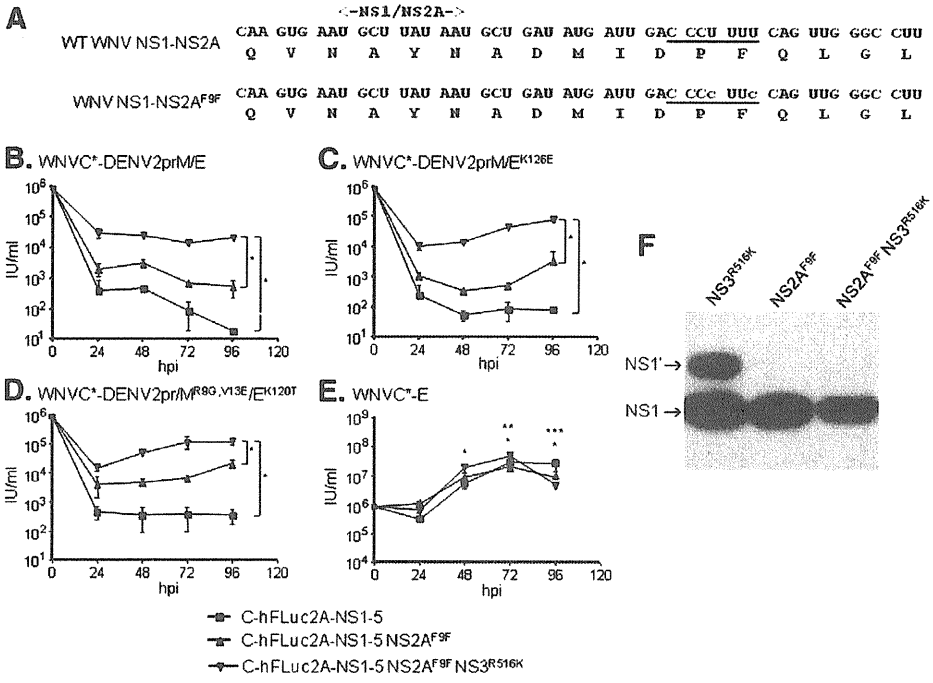

Fig. 5. Demonstration that ablation of ribosomal frame-shifting in NS2A enhances trans-encapsidation of WNV replicons and eliminates production of NS1'. (A) Alignment of RNA and amino acid sequences at the NS1/NS2A junction region of WNV showing the ribosomal frame-shift site (underlined) and its disruption by silent mutations. (B–E) Growth curves of VRPs harboring the WT replicon genomes, or genomes encoding the NS2A^{F9F} or NS2A^{F9F}NS3^{R516K} mutations on BHK cell lines encoding the indicated packaging constructs. Cell monolayers were infected at an MOI of 0.05 with the indicated VRPs, and media were harvested and titered at the indicated time points as described in the Materials and methods. The first time point (0 hpi) indicates the initial dose used to infect the cells. Values represent averages of two individual experiments. Error bars indicate standard deviation and "*" denotes significance as measured by two-way ANOVA with Bonferroni post-test ($p<0.05$) for 24–96 h timepoints (B and C) and 48–72 h timepoints (D). The same test showed significant differences in Fig. 5E; in this case: "*" denotes significance ($p<0.05$) for C-hFLuc2A-NS1-5 vs C-hFLuc2A-NS1-5NS2A^{F9F}NS3^{R516K}; "**" denotes significance ($p<0.05$) for C-hFLuc2A-NS1-5 NS2A^{F9F} vs C-hFLuc2A-NS1-5NS2A^{F9F}NS3^{R516K}; and "***" denotes significance ($p<0.05$) for C-hFLuc2A-NS1-5 vs C-hFLuc2A-NS1-5 NS2A^{F9F} at indicated timepoints. (F) Western blot showing that cells infected with VRPs containing the NS2A^{F9F} mutation fail to produce NS1'. Cells infected with particles encoding C-hFLuc2A-NS1-5 replicons encoding NS3^{R516K}, NS2A^{F9F}, or NS2A^{F9F} NS3^{R516K} mutations were lysed, blotted, and immunostained as described in the Materials and methods.

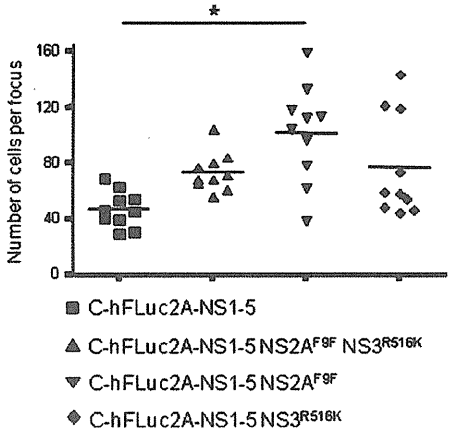

Fig. 6. Comparison of foci sizes of VRPs harboring the WT replicon genome, or genomes encoding the NS2A^{F9F}, NS2A^{F9F}NS3^{R516K} or NS3^{R516K} mutations on BHK(VEErep/WNVC*-E/Pac) cells expressing the WNV C-prM-E proteins. Cell monolayers were infected with serial dilutions of the VRPs, overlaid with semisolid medium, fixed, and immunostained with anti-NS1 antibody 48 h after incubation at 37 °C as described in the Materials and methods. The graph represents the counts of cells from 10 individual foci per VRP tested. The line represents the average of the 10 foci values for each group and "*" denotes significance as measured by one-way ANOVA with Bonferroni post-test ($p<0.001$).

these mutations during the adaptation of our dengue chimera to grow in cell culture. Furthermore, by comparing the specific infectivity of these preparations to those encoding envelopes of two encephalitic flaviviruses, we clearly demonstrated the poorer specific infectivity of particles encapsidated in DENV envelope proteins, consistent with work of Kuhn and co-workers documenting the poor specific infectivity of DENV2 virions (van der Schaar et al., 2007). Interaction among the proteins of positive-strand RNA viruses is one of the hallmarks of these viruses. Among the flaviviruses, numerous examples of such interactions exist within the structural proteins or within the well-defined non-structural protein complexes. Analyses of viable chimeras created from different species within the Flavivirus genus have revealed additional interactions. Several of these have documented interactions between components known to be involved in genome replication and the structural components of the virion. Among these, there has been a documented interaction of NS1 with the viral replicase via an interaction with NS4A (Lindenbach and Rice, 1999). In a previous report we demonstrated that adaptation of a DENV/WNV single-cycle chimeric flavivirus to grow to higher titers in a specifically designed packaging cell line resulted in the selection of mutations in NS2A and NS3. Here we definitively demonstrate that these mutations exert their growth-enhancing effect by interaction with the structural proteins, and that this growth enhancing effect is more pronounced in the context of DENV2 structural proteins. These data explain how these adaptations arose in response to the unnatural chimerization. In the case of the mutation in NS3, we were unable to define the mechanism by which this mutation was exerting its phenotype, but the ability of this mutation which lies within the helicase domain of NS3 to improve packaging of the viral genome supports previous evidence showing that changes in the helicase domain can alter encapsidation (Patkar and Kuhn, 2008).

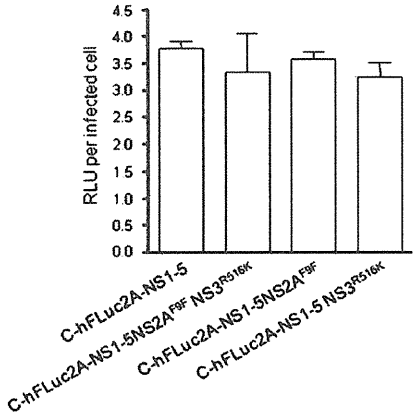

Fig. 7. Replication of VRPs harboring the WT replicon genome, or genomes encoding the NS2A^{F9F}, NS2A^{F9F}NS3^{R516K} or NS3^{R516K} mutations on BHK cells. Cells were cultured in 96-well plates, infected with VRPs and incubated for 24 h, when the relative luciferase units (RLU) were measured and then standardized to the number of VRP-infected cells obtained by immunostaining wells infected in a parallel plate (see Materials and methods). Data for each sample are averages of triplicate values with error bars showing standard deviations.

In the case of our NS2A mutation, which was found at codon 9 of the NS2A gene, we clearly demonstrate that this mutation functions through alteration of a recently documented ribosomal frame shift that produces an altered form of the NS1 protein (NS1') that is a characteristic of members of the JEV/WNV serocomplex of the flavivirus genus (Firth and Atkins, 2009; Mason, 1989; Melian et al., 2010). This interesting effect was evaluated by trans-complementation of genomes carrying the cell-adapted, non-synonymous mutation in NS2A which ablated the ribosome slippage site. These studies showed that this non-synonymous change increased transpackaging by prM/E proteins, and simultaneously eliminated the production of NS1'. The specific role of the frame shift in these phenotypes was confirmed by studies which demonstrated that synonymous mutations in this frame-shift site produced the same VRP growth-enhancing phenotype and ablation of NS1' production found in the non-synonymous mutation selected in our previous blind-passaging studies. Careful analyses of replicons harboring this mutation document that its effect on genome packaging, which was additive with the NS3 mutation, could be observed when packaging was evaluated in cells providing WNV or DENV2 prM/E coats. However, the growth-enhancing phenotype was more dramatic with the DENV2 prM/E coats, consistent with the hypothesis that these lower-specific infectivity coats provided a more significant selective pressure, allowing these mutations to arise in the chimeric background used for the initial passaging studies; the selection of these mutations is also consistent with preliminary studies showing that the combination of the NS2A frame-shift and NS3 point mutations into a replicon improve VRP yield from DENV E-producing cell lines by improving the specific infectivity of the resulting particles. Since the NS1 gene has been shown to serve a critical function in flavivirus genome replication we conducted studies to determine if ablation of NS1' by alteration of the slippage site could influence genome replication. These studies showed that abrogation of NS1' had no effect on genome replication, indicating that the mechanism by which NS1' alters particle packaging is due to an effect on virion assembly/release.

Our data demonstrating that the NS1' protein alters genome packaging expands the activities ascribed to the multifunctional NS1 protein. Although we have been unable to precisely determine how the larger form of the NS1 protein interferes with transpackaging of genomes into infectious particles, these findings are consistent with the slow egress of NS1 through the endoplasmatic reticulum (ER) of infected mammalian cells (Mason, 1989), the regulation of its localization to several compartments (Youn et al., 2010), the documented role of NS1 in genome replication (Muylaert et al., 1996; Muylaert et al., 1997), and interactions with NS4A (Lindenbach and Rice, 1999), all of which indicate that NS1 likely serves as a bridge between RNA synthesis and structural protein assembly. The finding that the extended form of NS1 has an inhibitory effect on virion packaging *in vitro* support this role. However, by themselves, these results are somewhat surprising. The fact that the effect on packaging was less pronounced in the presence of high-specific infectivity encephalitic flavivirus prM/E proteins is consistent with the fact that NS1' has

not been observed in other flaviviruses (see above). Interestingly, work by Khromykh and co-workers showed that abrogation of NS1' in a low-virulence isolate of WNV (Kunjin virus) reduced neurovirulence in mice (Melian et al., 2010). Although these studies did not document an effect of NS1' ablation on viral growth, they clearly showed an interesting effect of the NS1' protein *in vivo* but were unable to demonstrate any effect of the frame-shift ablation on growth of a mutant Kunjin virus *in vitro* in mammalian or insect cells (Melian et al., 2010). The inability to observe differences in growth of Kunjin viruses with or without the frame-shift mutation is consistent with our studies showing that productive growth of a single-cycle WNV (namely RepliVAX WN) in a complementing cell line was not improved by the introduction of this frame-shift mutation. Finally, although the influence of the frame shift on Kunjin virus neurovirulence may not provide an evolutionary advantage *per se*, the association of the frame-shift slippage site with the encephalitic flaviviruses likely reflects a selective biological advantage, which could be related to acquisition of additional functions by the larger form of NS1.

Materials and methods

Cells

BHK cells were maintained at 37 °C in minimal essential medium (MEM) supplemented with 10% fetal bovine serum (FBS) and antibiotics. Vero cells were maintained at 37 °C in MEM containing 6% FBS and antibiotics. BHK(VEErep/Pac-Ubi-C*) expressing the WNV C protein (Widman et al., 2008), BHK(VEErep/WNVC*-E/Pac) cells expressing the WNV C-prM-E proteins (Fayzulin et al., 2006), BHK(VEErep/WNC*-JEVprM-E/Pac) cells expressing the WNV C and JEV prM-E (Ishikawa et al., 2008), BHK(VEErep/WNVC*-DENV2prM/E/Pac) cells expressing the WNV C and the DENV2 NGC (low passage) prM/E (generated as described below), BHK(VEErep/WNVC*-DENV2prM/E^{K126E}/Pac) cells expressing the WNV C and a HS-binding E derived from a high-passage DENV2 NGC (generated as described below), and BHK(VEErep/WNVC*-DENV2pr/$M^{R9G,V13E}$/E^{K120T}/Pac) cells expressing the WNV C and the DENV2 prM/E mutations selected in RepliVAX D2 (generated as described below) were propagated at 37 °C in Dulbecco's MEM supplemented with 10% FBS and 10 μg/ml puromycin as previously described (Fayzulin et al., 2006).

Plasmid construction

The plasmid pWNR C-hFLuc2A NS1-5 encoding a WNV replicon expressing a hFLuc reporter gene has been previously described (Gilfoy et al., 2009). This was used to construct the various mutant WNV replicon plasmids with specific mutations in NS2A (pWNR C-hFLuc2A NS1-5 $NS2A^{S9F}$), NS3 (pWNR C-hFLuc2A CNS1-5 $NS3^{R516K}$), NS2A and NS3 (pWNR C-hFLuc2A NS1-5 $NS2A^{S9F}$/$NS3^{R516K}$), as well as a silent mutation in NS2A (pWNR C-hFLuc2A NS1-5 $NS2A^{F9F}$) using standard techniques (Higuchi et al., 1988).

The plasmid encoding the RepliVAX WN replicon [pRepliVAX WN (Widman et al., 2008); previously referred to as pRepliVAX WN.2 SP] was modified using standard techniques to produce a series of mutant RepliVAX WN plasmids with specific mutations in NS2A (pRepliVAX WN $NS2A^{S9F}$), NS3 (pRepliVAX WN $NS3^{R516K}$), and NS2A and NS3 (pRepliVAX WN $NS2A^{S9F}$/$NS3^{R516K}$) using standard techniques (Higuchi et al., 1988).

Plasmid pVEErep/WNVC*-E/Pac which encodes a Venezuelan equine encephalitis virus replicon (VEErep) capable of persisting in cells in the presence of puromycin and expressing the WNV structural proteins (C-prM-E) needed to package subgenomic replicons (Fayzulin et al., 2006) was used to construct a series of plasmids encoding a low-passage DENV2 NGC (Fonseca, 1994) prM/E cassette (pVEErep/WNVC*-DENV2prM/E/Pac), a high-passage DENV2 NGC (Fonseca, 1994) prM/E cassette (pVEErep/WNVC*-DENV2prM/E^{K126E}/Pac), or the prM/E cassette found in cell-adapted RepliVAX D2 (Suzuki et al., 2009) (pVEErep/WNVC*-DENV2pr/$M^{R9G,V13E}$/E^{K120T}/Pac). Sequences of all constructs are available from the authors upon request.

Production of packaging cell lines

Cell lines harboring replicons from the VEErep plasmids were created by a slight modification of the previously described procedures (Fayzulin et al., 2006). Briefly, the plasmid DNAs were linearized by using the MluI restriction enzyme, and the resulting template DNAs were *in vitro*-transcribed using MegaScript SP6 synthesis kit (Ambion) in the presence of 7mG(ppp)G cap analog (New England Biolabs). The yield and integrity of transcripts were determined by using non-denaturing gel electrophoresis, aliquots of transcription reactions were transfected into BHK cells using Lipofectin (Invitrogen), VEErep-harboring cell lines were selected in the presence of puromycin, and clones displaying high-level expression of these replicons were isolated and propagated using standard techniques.

Production of VRPs and RepliVAX WN derivatives

WNV replicon RNAs encoding the hFLuc gene (WNR C-hFLuc2A NS1-5 and derivatives) or the WNV prM/E cassette (RepliVAX WN and derivatives) were generated by using MegaScript T7 synthesis kit (Ambion) and 7mG(ppp)G cap analog (New England Biolabs) from SwaI-linearized templates created from the relevant plasmid DNAs using standard methods. Following analysis for yield and integrity as described above, aliquots of transcription reactions were electroporated into packaging cell lines (expressing C, prM, and E constructs in the case of the hFLuc-expressing replicon constructs or C only in the case of RepliVAX constructs) and then collected as previously described (Fayzulin et al., 2006).

VRP and RepliVAX titrations

VRPs and RepliVAX WN derivatives were titrated on Vero cells as previously described (Fayzulin et al., 2006). Yields are reported as infectious units per milliliter (IU/ml).

VRP and RepliVAX growth curves

To compare growth properties of the various WNV replicons in cell lines encoding various prM/E packaging constructs, VRPs derived from electroporations were used to infect these BHK packaging cells at a multiplicity of infection (MOI) of 0.05 for 2 h, the monolayers were washed 3 times (5 min each) with MEM supplemented with 1% FBS, 10 mM HEPES, and antibiotics, and the cultures were placed at 37 °C. Media were removed and replaced with fresh media at the indicated time points and stored at −80 °C for subsequent titration as described above.

Growth curves from RepliVAX WN and derivatives were prepared by infecting BHK(VEErep/Pac-Ubi-C*) cells at an MOI of 0.01 using the same procedure as described above.

Specific infectivity studies

Genome copy numbers and infectivity of VRPs produced by electroporation (see above) were determined based on semiquantitative PCR and Vero cell titration data. Briefly, VRP preparations were diluted to give titers of 1000 IU/ml, and one portion was titered on Vero cells as described above, while RNA was isolated from a second portion using the QIAamp Viral RNA kit (QIAGEN) following the manufacturer's protocol. The viral RNA concentration in this sample was determined by using a semiquantitative PCR (sqPCR) assay in which serial 2-fold dilutions of RNA from each sample were used for reverse transcription (RT) carried out with an ImProm II RT kit (Promega)

with random hexamers followed by amplification of a 100 bp PCR product using previously described WNV NS5-specific primers (Bourne et al., 2007). The PCR conditions included an initial cycle of 5 min at 95 °C, 30 cycles of 30 s at 95 °C, 30 s at 53 °C and 30 s at 72 °C, followed by 5 min at 72 °C. Following amplification, the PCR products were resolved by electrophoresis on 2% agarose gels containing 200 ng/ml of ethidium bromide, and images of the gels were acquired with a CCD camera using a FluorChem 8900 Chemiluminescence Gel Imager (Alpha Innotech) and band intensities were quantified by using ImageJ software (available at http://rsbweb.nih.gov/ij/). The intensities of these bands were compared to a standard curve generated with known numbers of genome copies of *in vitro* synthesized RNA from WNR C-hFLuc2A NS1-5 (ranging from 2000 to 200,000 copies), and the resulting standard curve (generated by using GraphPad Prism 4 software) (Fig. S1) was used to calculate the genome copies in each test sample. The specific infectivities of each preparation were then calculated by dividing this genome copy number per IU in the same sample volume, giving genome copies/IU of each VRP.

Western blot analyses of NS1

VRPs containing different derivatives of WNR C-hFLuc2A NS1-5 were inoculated onto BHK cell monolayers at an MOI of 5 and incubated at 37 °C with serum-free medium (OptiPro SFM, Gibco) supplemented with 10 mM HEPES and antibiotics. At 24 h after infection, culture fluids were collected and cell lysates were prepared using lysis buffer (0.1% Triton X-100, 300 mM NaCl, 50 mM Tris–HCl; pH 7.6) containing a protease inhibitor cocktail (Roche). Samples were resolved on 4–12% gradient Bis–Tris polyacrylamide gels (Invitrogen) and transferred to polyvinyldene diofluoride membranes, which were then incubated with a 1:5000 dilution of a mouse anti-NS1 antibody from hydridoma JE-6H4 (Kitai et al., 2007). Following washing, the membranes were incubated with a 1:10,000 dilution of peroxidase-conjugated anti-mouse IgG (KPL), and the bound peroxidase was visualized by using ECL Plus System (GE healthcare).

VRP focus-formation assay

To compare focus morphology, monolayers of BHK(VEErep/WNVC*-E/Pac) cells expressing the WNV C-prM-E proteins were infected with serial dilutions of VRPs harboring the WT replicon genome, or genomes encoding the $NS2A^{F9F}$, $NS2A^{F9F}NS3^{R516K}$ or $NS3^{R516K}$ mutations. Following absorption for 2 h, the cells were overlaid with medium containing 0.8% carboxymethyl cellulose (CMC) (Sigma, Saint Louis, MO) supplemented with 1% FBS, 10 mM HEPES and antibiotics and incubated at 37 °C for 48 h. To visualize foci, the cells were fixed with 50% acetone–50% methanol solution followed by incubation with a 1:5000 dilution of a mouse anti-NS1 antibody from hybridoma JE-6H4 (Kitai et al., 2007), peroxidase conjugated anti-mouse IgG (KPL, Gaithersburg, MD) and VIP substrate (Vector Laboratories, Burlingame, CA). The number of cells forming individualized focus was counted and used to compare focus size.

Luciferase assay

BHK monolayers prepared in 96-well black-wall plates were infected with dilutions of VRPs harboring the WT replicon genome, or genomes encoding the $NS2A^{F9F}$, $NS2A^{F9F}NS3^{R516K}$ or $NS3^{R516K}$ mutations and incubated at 37 °C. At 24 h post infection, an equal volume of 25% Steady-Glo Luciferase Assay System reagent (Promega) diluted in lysis buffer was added to the cells and incubated for 5 min on rocker to allow cell lysis. The luminescence was measured on a Microplate Luminometer (Applied Biosystems, Foster City, CA). A parallel plate infected with the same dilutions of VRPs was harvested at 24 h post infection and used to determine the number of VRP-infected cells determined by immunostaining (as described above). The luciferase activity was normalized by the number of VRP-infected cells and expressed as relative luciferase units (RLU) per infected cell.

Statistical analyses

GraphPad Prism (GraphPad Software, San Diego, CA) was used to analyze data. One-way or two-way analysis of variance (ANOVA) with the Bonferroni post-test were used where appropriate. P values less than 0.05 were considered to indicate statistical significance.

Acknowledgments

We thank T. Ishikawa (Kobe University) for helpful discussion concerning NS1' detection and E. Konishi (Kobe University) for supplying the JE-6H4 monoclonal antibody. This work was supported by a grant from NIAID to PWM through the Western Regional Center of Excellence for Biodefense and Emerging Infectious Disease Research (NIH grant number U54 AI057156), NIH grants R21 AI077077 and UO1 AI082960 and a grant from the Sealy Center for Vaccine Development (SCVD). ERW was supported by a SCVD Predoctoral Fellowship for a portion of these studies.

Appendix A. Supplementary data

Supplementary data to this article can be found online at doi:10.1016/j.virol.2011.09.007.

References

Alcon, S., Talarmin, A., Debruyne, M., Falconar, A., Deubel, V., Flamand, M., 2002. Enzyme-linked immunosorbent assay specific to Dengue virus type 1 nonstructural protein NS1 reveals circulation of the antigen in the blood during the acute phase of disease in patients experiencing primary or secondary infections. J. Clin. Microbiol. 40 (2), 376–381.

Anez, G., Men, R., Eckels, K.H., Lai, C.J., 2009. Passage of dengue virus type 4 vaccine candidates in fetal rhesus lung cells selects heparin-sensitive variants that result in loss of infectivity and immunogenicity in rhesus macaques. J. Virol. 83 (20), 10384–10394.

Bourne, N., Scholle, F., Silva, M.C., Rossi, S.L., Dewsbury, N., Judy, B., De Aguiar, J.B., Leon, M.A., Estes, D.M., Fayzulin, R., Mason, P.W., 2007. Early production of type I interferon during West Nile virus infection: role for lymphoid tissues in IRF3-independent interferon production. J. Virol. 81 (17), 9100–9108.

Fan, W.F., Mason, P.W., 1990. Membrane association and secretion of the Japanese encephalitis virus NS1 protein from cells expressing NS1 cDNA. Virology 177 (2), 470–476.

Fayzulin, R., Scholle, F., Petrakova, O., Frolov, I., Mason, P.W., 2006. Evaluation of replicative capacity and genetic stability of West Nile virus replicons using highly efficient packaging cell lines. Virology 351 (1), 196–209.

Firth, A.E., Atkins, J.F., 2009. A conserved predicted pseudoknot in the NS2A-encoding sequence of West Nile and Japanese encephalitis flaviviruses suggests NS1' may derive from ribosomal frameshifting. Virol. J. 6, 14.

Fonseca, B.A.L., 1994. Vaccinia-vectored dengue vaccine candidates elicit neutralizing antibodies in mice. Doctoral thesis. Yale University, New Haven, CT.

Gilfoy, F., Fayzulin, R., Mason, P.W., 2009. West Nile virus genome amplification requires the functional activities of the proteasome. Virology 385 (1), 74–84.

Halstead, S.B., Thomas, S.J., 2011. New Japanese encephalitis vaccines: alternatives to production in mouse brain. Expert Rev. Vaccines 10 (3), 355–364.

Higuchi, R., Krummel, B., Saiki, R.K., 1988. A general method of in vitro preparation and specific mutagenesis of DNA fragments: study of protein and DNA interactions. Nucleic Acids Res. 16 (15), 7351–7367.

Ishikawa, T., Widman, D.G., Bourne, N., Konishi, E., Mason, P.W., 2008. Construction and evaluation of a chimeric pseudoinfectious virus vaccine to prevent Japanese encephalitis. Vaccine 26 (22), 2772–2781.

Junjhon, J., Edwards, T.J., Utaipat, U., Bowman, V.D., Holdaway, H.A., Zhang, W., Keelapang, P., Puttikhunt, C., Perera, R., Chipman, P.R., Kasinrerk, W., Malasit, P., Kuhn, R.J., Sittisombut, N., 2010. Influence of pr-M cleavage on the heterogeneity of extracellular dengue virus particles. J. Virol. 84 (16), 8353–8358.

Kitai, Y., Shoda, M., Kondo, T., Konishi, E., 2007. Epitope-blocking enzyme-linked immunosorbent assay to differentiate West Nile virus from Japanese encephalitis virus infections in equine sera. Clin. Vaccine Immunol. 14 (8), 1024–1031.

Konishi, E., Pincus, S., Fonseca, B.A., Shope, R.E., Paoletti, E., Mason, P.W., 1991. Comparison of protective immunity elicited by recombinant vaccinia viruses that synthesize E or NS1 of Japanese encephalitis virus. Virology 185 (1), 401–410.

Kroschewski, H., Allison, S.L., Heinz, F.X., Mandl, C.W., 2003. Role of heparan sulfate for attachment and entry of tick-borne encephalitis virus. Virology 308 (1), 92–100.

Lee, E., Lobigs, M., 2000. Substitutions at the putative receptor-binding site of an encephalitic flavivirus alter virulence and host cell tropism and reveal a role for glycosaminoglycans in entry. J. Virol. 74 (19), 8867–8875.